Supporting Information

Mechanical Interlocking of 144 Symmetrical ^{19}F and Tetraphenylethylene for Magnetic Resonance-Fluorescence Dual Imaging

Lan Yang,[ǂ, §, #] Fang Wang,[§, #] Yu Li,[§, #] Rui Zhou,[§] Anfeng Li,[§] Tingjuan Wu,[§] Maosong Qiu,[§] Lei Zhang,[§] Minghui Yang,[§] Xin Zhou,[§, ǁ] Zhong-Xing Jiang,[*, ǂ, §, ǁ] and Shizhen Chen[*, §, ǁ]

ǂ School of Pharmaceutical Sciences, Wuhan University, Wuhan 430071, China.

§ State Key Laboratory of Magnetic Resonance Spectroscopy and Imaging, National Center for Magnetic Resonance in Wuhan, Wuhan Institute of Physics and Mathematics, Innovation Academy for Precision Measurement Science and Technology, Chinese Academy of Sciences, Wuhan 430071, China.

ǁ University of Chinese Academy of Sciences, Beijing 100049, China.

# L.Y., F.W., and Y.L. contributed equally to this work.

Email: Jiang Z.-X. zxjiang@apm.ac.cn, Chen S. chenshizhen@apm.ac.cn

Table of Contents

1. General Information

Unless otherwise mentioned, all solvents and reagents were purchased from commercial sources and used without further purification. Chromatographic purification of products was accomplished by flash chromatography using silica gel. Thin-layer chromatography (TLC) was performed on Silicycle 250 mm silica gel HSGF-254 plates (Yantai Jiangyou Silicon Gel Development Co.). ^{1}H, ^{13}C, and ^{19}F NMR spectra and relaxation time (T_1 and T_2) were recorded on Bruker 500 MHz or 600 MHz spectrometers. Chemical shifts were in ppm and coupling constants (J) were in Hertz (Hz). ^{1}H NMR spectra were referenced to deuterated solvents (J&K Scientific Ltd.), including $CDCl_3$ (s, 7.26 ppm), CD_3CN (s, 1.94 ppm), DMSO-d_6 (s, 2.50 ppm) and THF-d_8 (m, 17.2 ppm and 3.58 ppm). ^{13}C NMR spectra were referenced to solvent carbons (1.32 ppm for CD_3CN. ^{19}F NMR spectra were referenced to 2% perfluorobenzene (s, -164.90 ppm) or CF_3SO_3Na (s, -79.60 ppm) in deuterated solvents. The splitting patterns for ^{1}H NMR spectra were denoted as follows: s (singlet), d (doublet), t (triplet), q (quartet), m (multiplet), br (broad), and combinations thereof. High-resolution mass spectra (HRMS) were recorded on a Thermo Fisher Scientific Q Exactive Focus. MALDI-TOF mass spectra were recorded on a Bruker Ultraflex TOF-MS using the single MS mode for positive ions. UV-vis absorption spectra were recorded on Thermo Scientific Evolution 220 UV-visible Spectrophotometer. The fluorescence emission spectra and the fluorescence lifetime were recorded on Horiba Scientific Fluoromax-4 Spectrofluorometer, the excitation wavelength is 330 nm and the slit width is 5 nm for fluorescence emission spectra, the NanoLED-280 was used as the light source for fluorescence lifetime. The absolute fluorescence quantum yield was recorded on the FLS1000 Photoluminescence Spectrometer. The SEM was recorded on Zeiss SIGMA.

2. Supplementary Figures and Tables

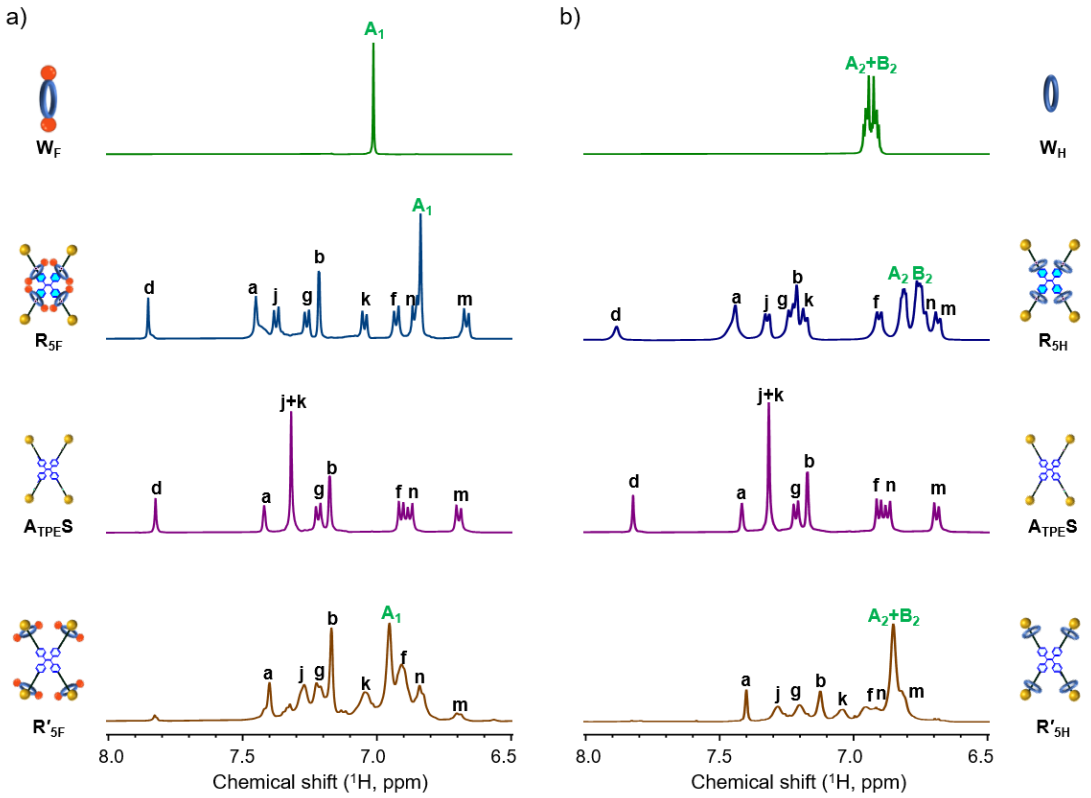

Figure S1. Partial enlarged ^{1}H NMR spectra of $\mathbf{W_F}$, $\mathbf{R_{5F}}$, $\mathbf{A_{TPE}S}$, and $\mathbf{R'_{5F}}$ (a) and $\mathbf{W_H}$, $\mathbf{R_{5H}}$, $\mathbf{A_{TPE}S}$, and $\mathbf{R'_{5H}}$ (b).

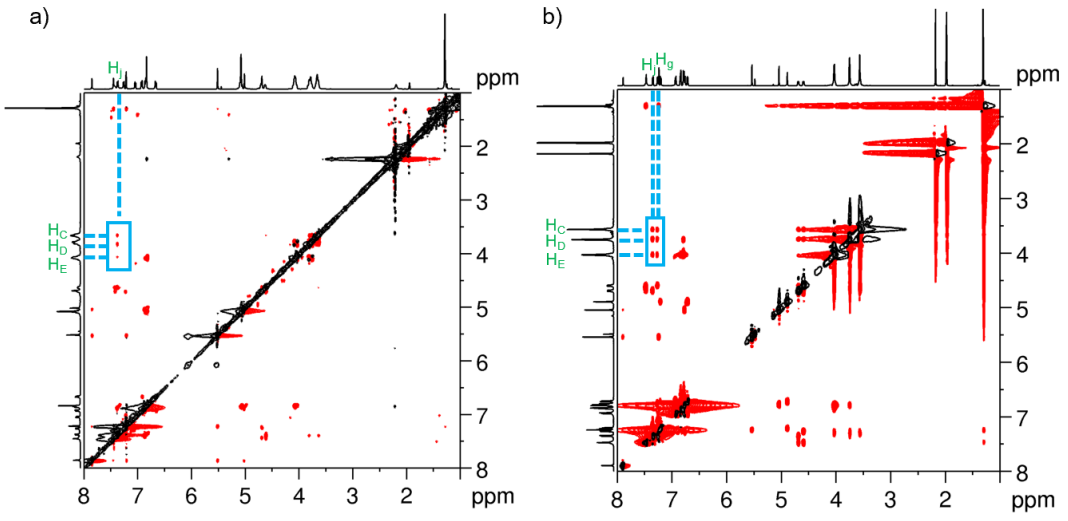

Figure S2. ^{1}H-^{1}H ROESY NMR spectra of $\mathbf{R_{5F}}$ (a) and $\mathbf{R_{5H}}$ (b). Conditions: 2.5 mM in CD_3CN at 298 K recorded on a 600 MHz NMR spectrometer.

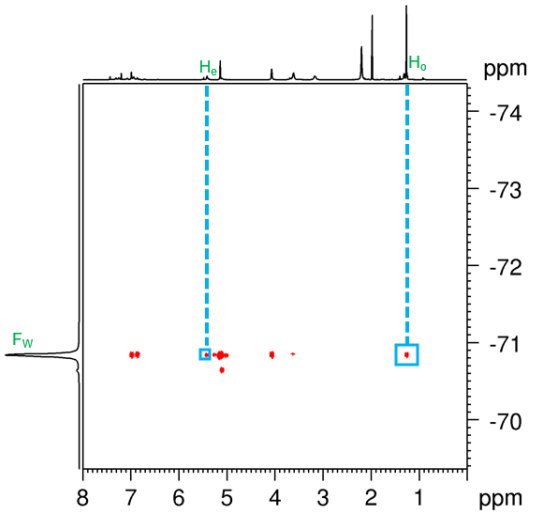

Figure S3. ^{1}H-^{19}F HOESY NMR spectrum of **R′$_{5F}$**. Conditions: 2.5 mM in CD_3CN at 298 K recorded on a 600 MHz NMR spectrometer.

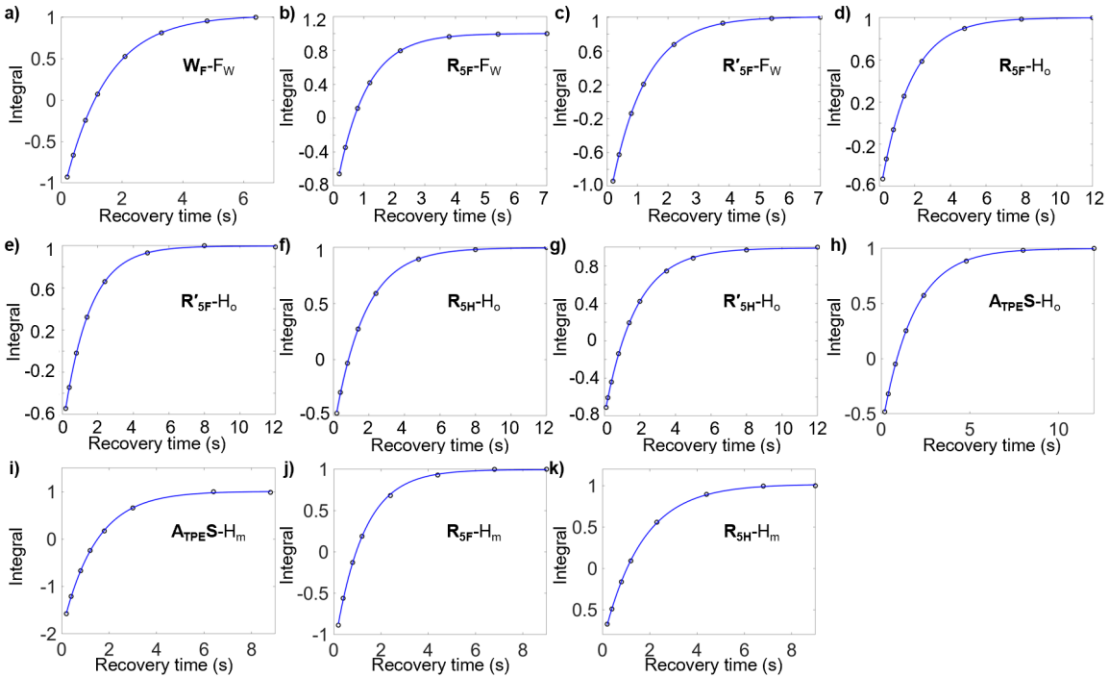

Figure S4. One of the representative fitting curves for T_1 of **W$_F$**, **R$_{5F}$**, **R′$_{5F}$**, **R$_{5H}$**, **R′$_{5H}$** and **A$_{TPE}$S** from 3 repetitions.

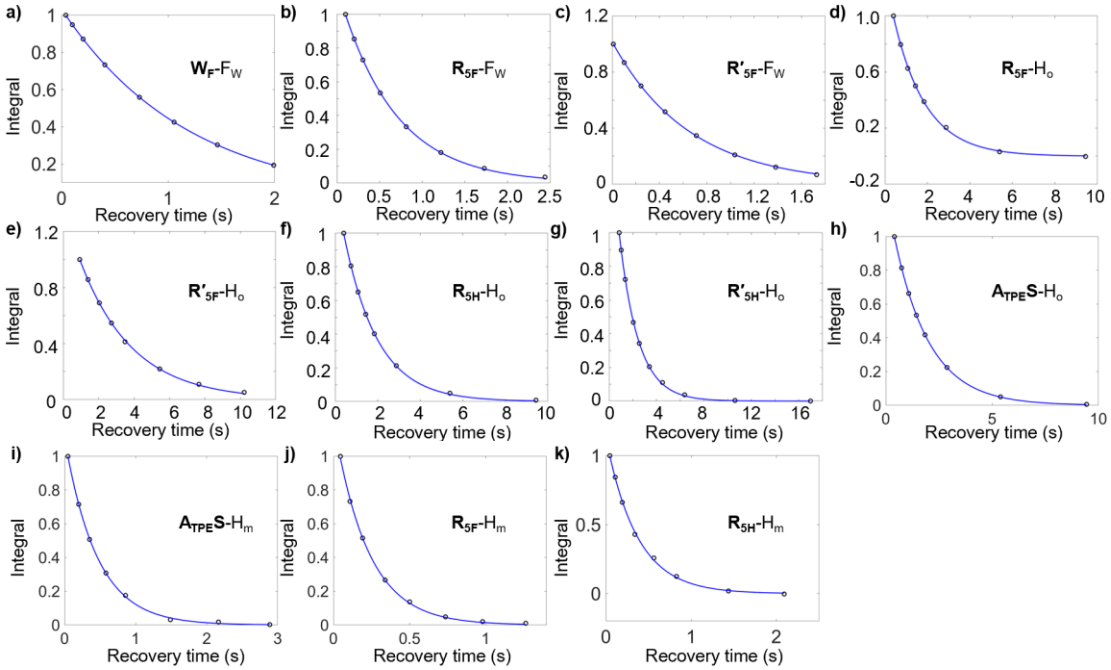

Figure S5. One of the representative fitting curves for T_2 of $\mathbf{W_F}$, $\mathbf{R_{5F}}$, $\mathbf{R'_{5F}}$, $\mathbf{R_{5H}}$, $\mathbf{R'_{5H}}$ and $\mathbf{A_{TPE}S}$ from 3 repetitions.

Table S1. Fitting results of F_w in $\mathbf{W_F}$, $\mathbf{R_{5F}}$, and $\mathbf{R'_{5F}}$

Compounds	$\mathbf{W_F}$			$\mathbf{R_{5F}}$			$\mathbf{R'_{5F}}$		
T_1 (s)	1.391	1.389	1.392	0.954	0.957	0.952	1.000	1.000	0.998
T_1 (s) mean ± SD	**1.391 ± 0.0012**			**0.954 ± 0.0021**			**0.999 ± 0.0009**		
T_2 (s)	1.193	1.189	1.188	0.648	0.644	0.645	0.697	0.687	0.654
T_2 (s) mean ± SD	**1.190 ± 0.0024**			**0.646 ± 0.0016**			**0.679 ± 0.0184**		
R_1 (s^{-1})	0.719	0.720	0.718	1.048	1.045	1.050	1.000	1.000	1.002
R_1 (s^{-1}) mean ± SD	**0.719 ± 0.0006**			**1.048 ± 0.0023**			**1.001 ± 0.0009**		
R_2 (s^{-1})	0.838	0.842	0.840	1.543	1.553	1.550	1.435	1.456	1.529
R_2 (s^{-1}) mean ± SD	**0.840 ± 0.0017**			**1.549 ± 0.0039**			**1.473 ± 0.0404**		

Table S2. Fitting results of H_o in **R′$_{5F}$**, **R$_{5F}$**, and **A$_{TPE}$S**

Compounds	**R′$_{5F}$**			**R$_{5F}$**			**A$_{TPE}$S**		
T_1 (s)	1.531	1.511	1.524	1.681	1.696	1.694	1.808	1.761	1.776
***T*$_1$ (s) mean ± SD**	**1.522 ± 0.0083**			**1.690 ± 0.0066**			**1.782 ± 0.0196**		
T_2 (s)	1.425	1.409	1.447	1.599	1.624	1.601	1.580	1.65	1.605
***T*$_2$ (s) mean ± SD**	**1.427 ± 0.0157**			**1.608 ± 0.0111**			**1.612 ± 0.0299**		
R_1 (s^{-1})	0.653	0.662	0.656	0.595	0.590	0.590	0.553	0.568	0.563
***R*$_1$ (s^{-1}) mean ± SD**	**0.657 ± 0.0036**			**0.592 ± 0.0023**			**0.561 ± 0.0061**		
R_2 (s^{-1})	0.702	0.710	0.691	0.625	0.616	0.625	0.633	0.605	0.623
***R*$_2$ (s^{-1}) mean ± SD**	**0.701 ± 0.0077**			**0.622 ± 0.0043**			**0.620 ± 0.0114**		

Table S2 (continued). Fitting results of H_o in **R$_{5H}$**, and **R′$_{5H}$**

Compounds	**R$_{5H}$**			**R′$_{5H}$**		
T_1 (s)	1.707	1.670	1.711	1.543	1.575	1.565
***T*$_1$ (s) mean ± SD**	**1.696 ± 0.0185**			**1.561 ± 0.0134**		
T_2 (s)	1.609	1.638	1.597	1.398	1.449	1.470
***T*$_2$ (s) mean ± SD**	**1.614 ± 0.0170**			**1.439 ± 0.0303**		
R_1 (s^{-1})	0.586	0.599	0.584	0.648	0.635	0.639
***R*$_1$ (s^{-1}) mean ± SD**	**0.590 ± 0.0065**			**0.641 ± 0.0055**		
R_2 (s^{-1})	0.622	0.611	0.626	0.715	0.690	0.680
***R*$_2$ (s^{-1}) mean ± SD**	**0.619 ± 0.0065**			**0.695 ± 0.0148**		

Table S3. Fitting results of H_m in **R$_{5F}$**, **A$_{TPE}$S**, and **R$_{5H}$**

Compounds	**R$_{5F}$**			**A$_{TPE}$S**			**R$_{5H}$**		
T_1 (s)	1.136	1.159	1.199	1.336	0.349	1.402	1.630	1.629	1.634
***T*$_1$ (s) mean ± SD**	**1.165 ± 0.0260**			**1.362 ± 0.0285**			**1.631 ± 0.0022**		
T_2 (s)	0.219	0.220	0.226	0.456	0.451	0.451	0.367	0.355	0.365
***T*$_2$ (s) mean ± SD**	**0.222 ± 0.0031**			**0.453 ± 0.0024**			**0.362 ± 0.0053**		
R_1 (s^{-1})	0.880	0.863	0.834	0.749	0.741	0.713	0.613	0.614	0.612
***R*$_1$ (s^{-1}) mean ± SD**	**0.859 ± 0.0191**			**0.734 ± 0.0152**			**0.613 ± 0.0008**		
R_2 (s^{-1})	4.558	4.554	4.424	2.194	2.220	2.216	2.728	2.821	2.743
***R*$_2$ (s^{-1}) mean ± SD**	**4.511 ± 0.0765**			**2.210 ± 0.0115**			**2.763 ± 0.0406**		

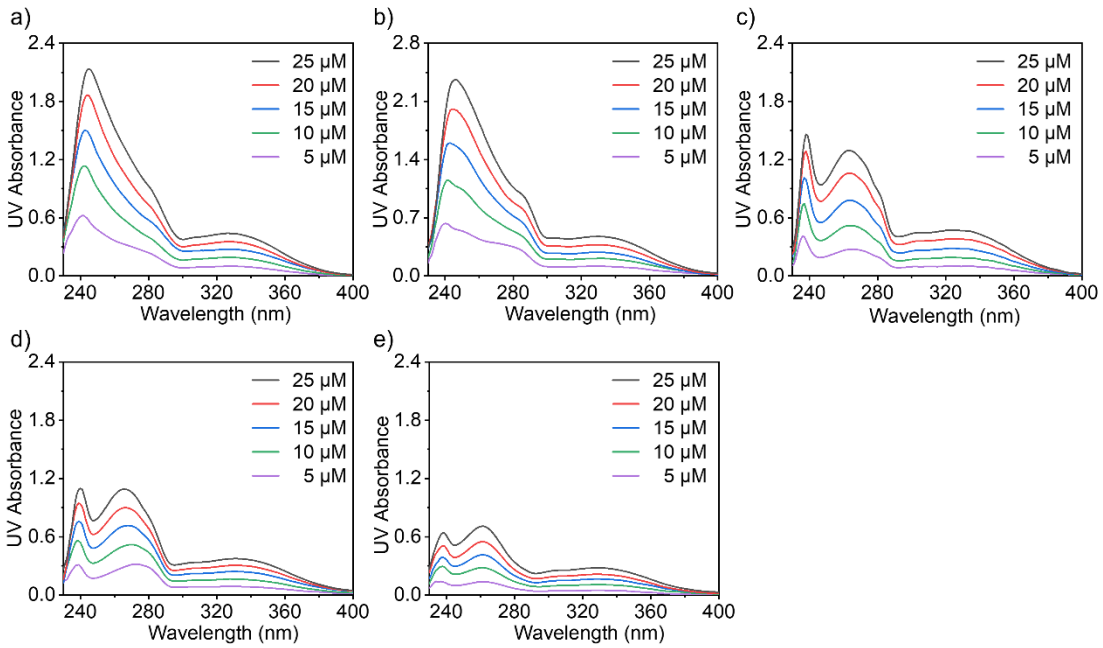

Figure S6. Concentration-dependent UV absorption spectra of $\mathbf{R_{5F}}$ (a), $\mathbf{R'_{5F}}$ (b), $\mathbf{R_{5H}}$ (c), $\mathbf{R'_{5H}}$ (d), and $\mathbf{A_{TPE}S}$ (e) in THF.

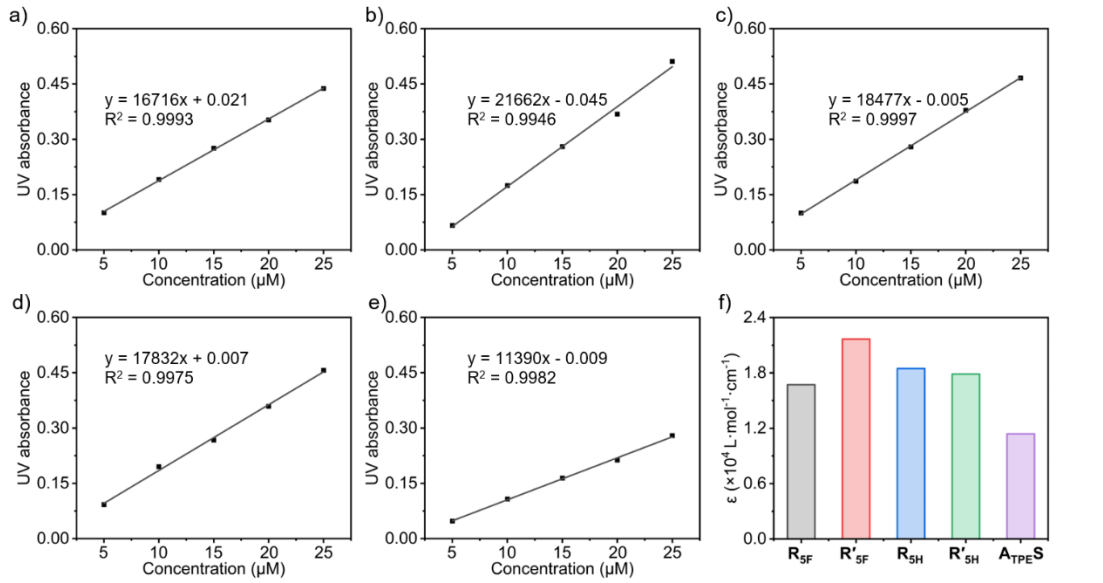

Figure S7. Fitted linear relationship between the absorbance (330 nm) and concentration of $\mathbf{R_{5F}}$ (a), $\mathbf{R'_{5F}}$ (b), $\mathbf{R_{5H}}$ (c), $\mathbf{R'_{5H}}$ (d), and $\mathbf{A_{TPE}S}$ (e), and the corresponding molecular extinction coefficients (ε) in THF (f).

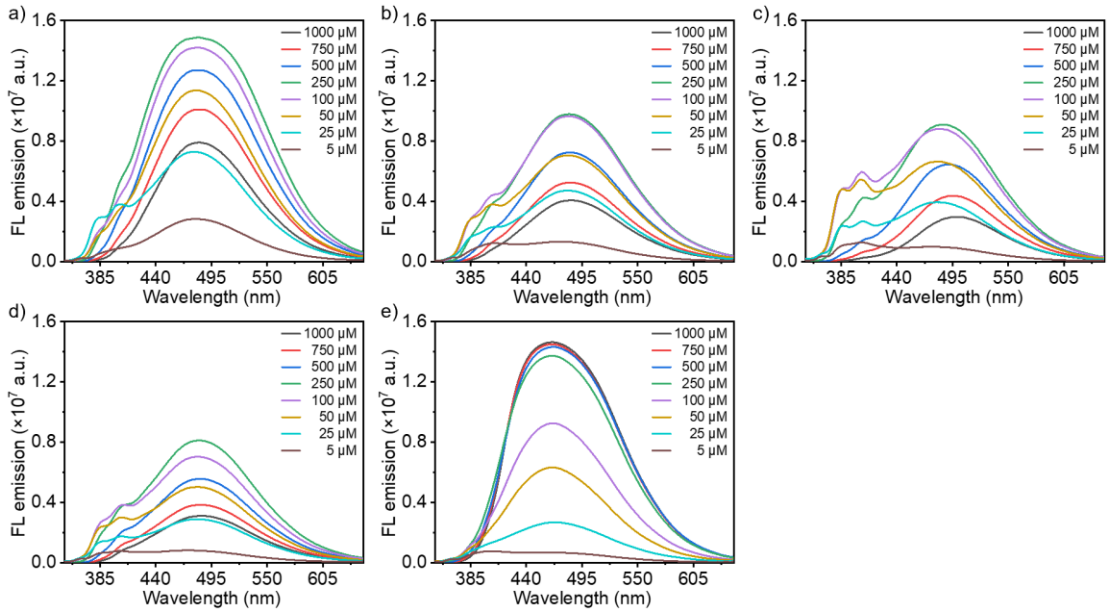

Figure S8. Concentration-dependent FL emission spectra of $\mathbf{R_{5F}}$ (a), $\mathbf{R'_{5F}}$ (b), $\mathbf{R_{5H}}$ (c), $\mathbf{R'_{5H}}$ (d) and $\mathbf{A_{TPE}S}$ (e) in THF.

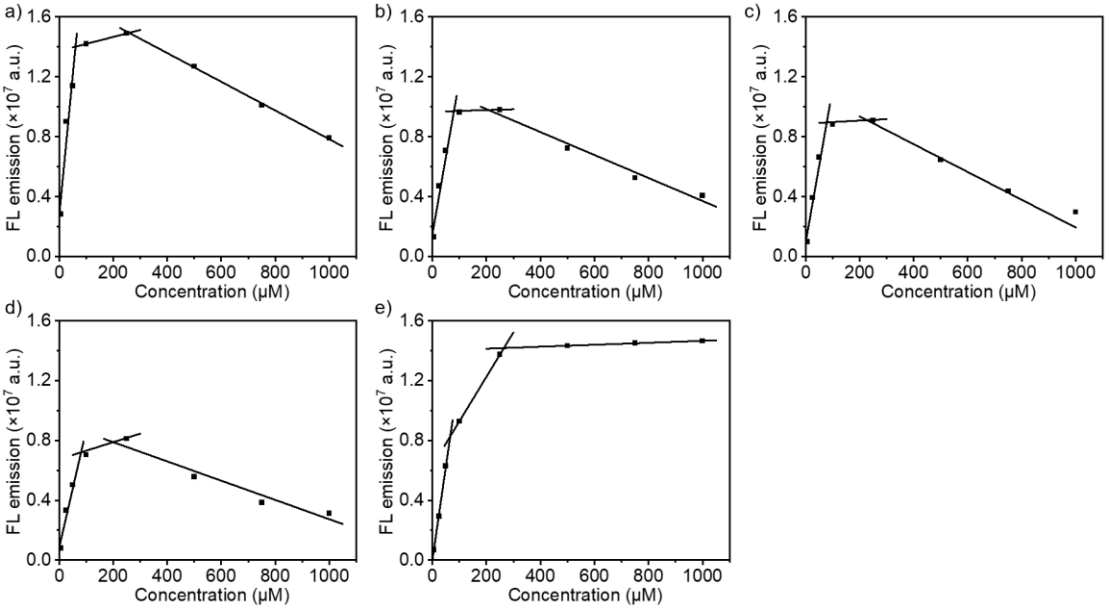

Figure S9. Fitted concentration-dependent maximum FL intensity curves of $\mathbf{R_{5F}}$ (a), $\mathbf{R'_{5F}}$ (b), $\mathbf{R_{5H}}$ (c), $\mathbf{R'_{5H}}$ (d), and $\mathbf{A_{TPE}S}$ (e) in THF.

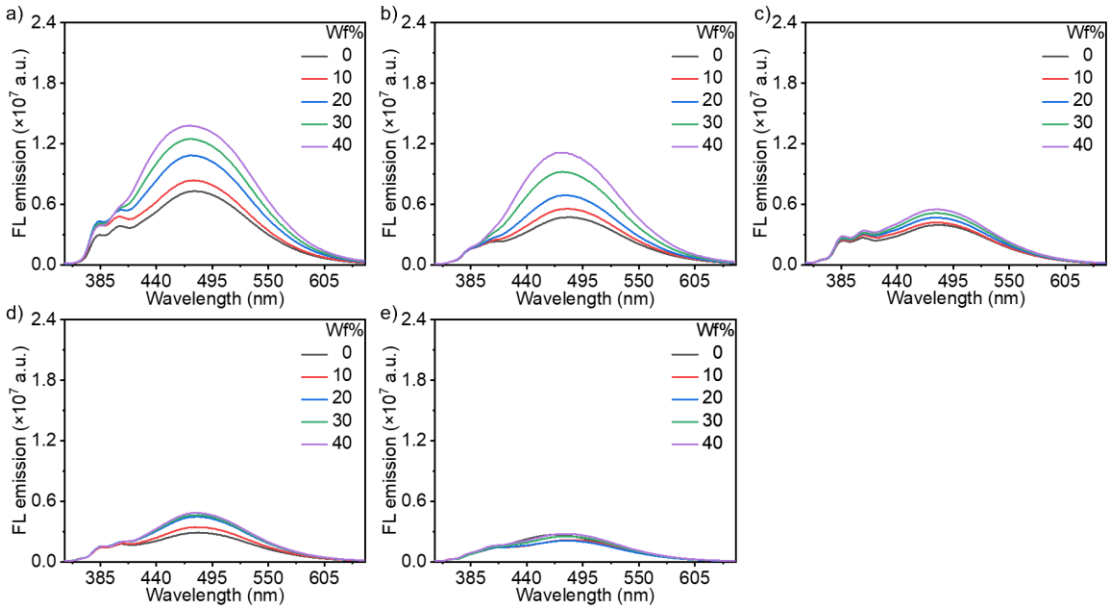

Figure S10. FL emission spectra of $\mathbf{R_{5F}}$ (a), $\mathbf{R'_{5F}}$ (b), $\mathbf{R_{5H}}$ (c), $\mathbf{R'_{5H}}$ (d), and $\mathbf{A_{TPE}S}$ (e) in a mixture of water and THF at the indicated ratios. Concentration: 25 μM

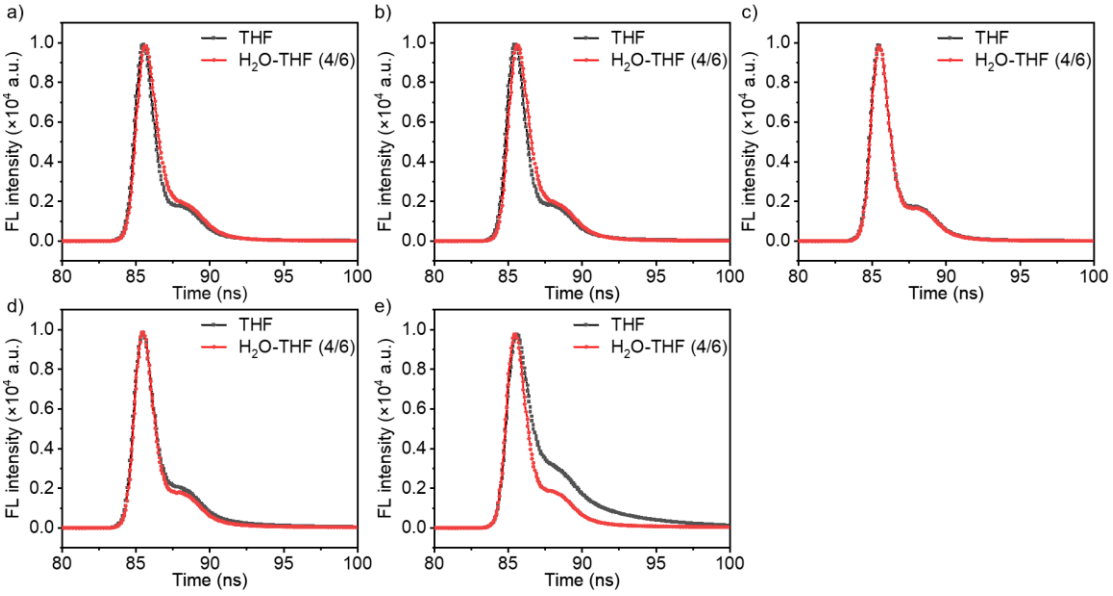

Figure S11. Time-resolution photoluminescence spectra of $\mathbf{R_{5F}}$ (a), $\mathbf{R'_{5F}}$ (b), $\mathbf{R_{5H}}$ (c), $\mathbf{R'_{5H}}$ (d), and $\mathbf{A_{TPE}S}$ (e) at the indicated water contents in THF solution. Concentration: 25 μM.

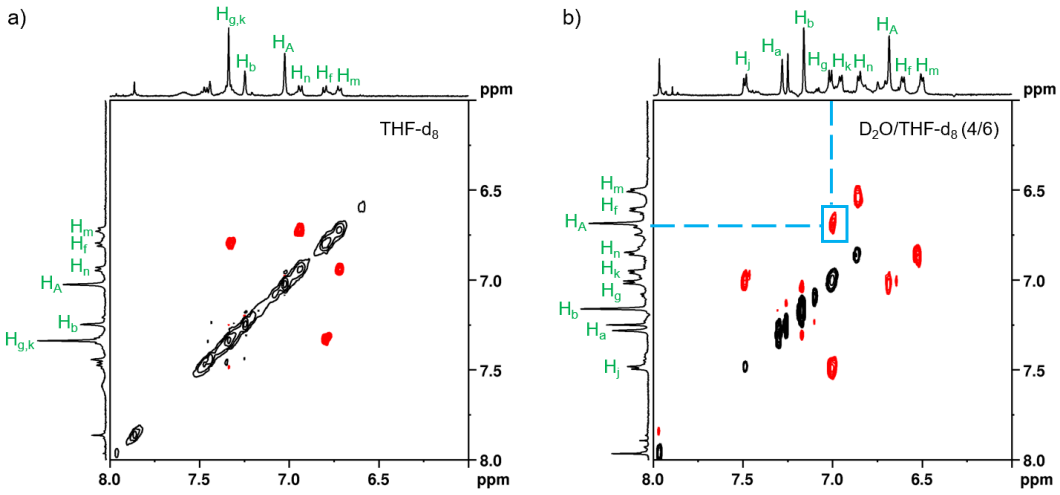

Figure S12. ^{1}H-^{1}H ROESY NMR spectra of **R_{5F}** in THF-d_8 (a) and D_2O/THF-d_8 (4:6) (b). Conditions: 25 μM, 298 K, 600 MHz NMR spectrometer.

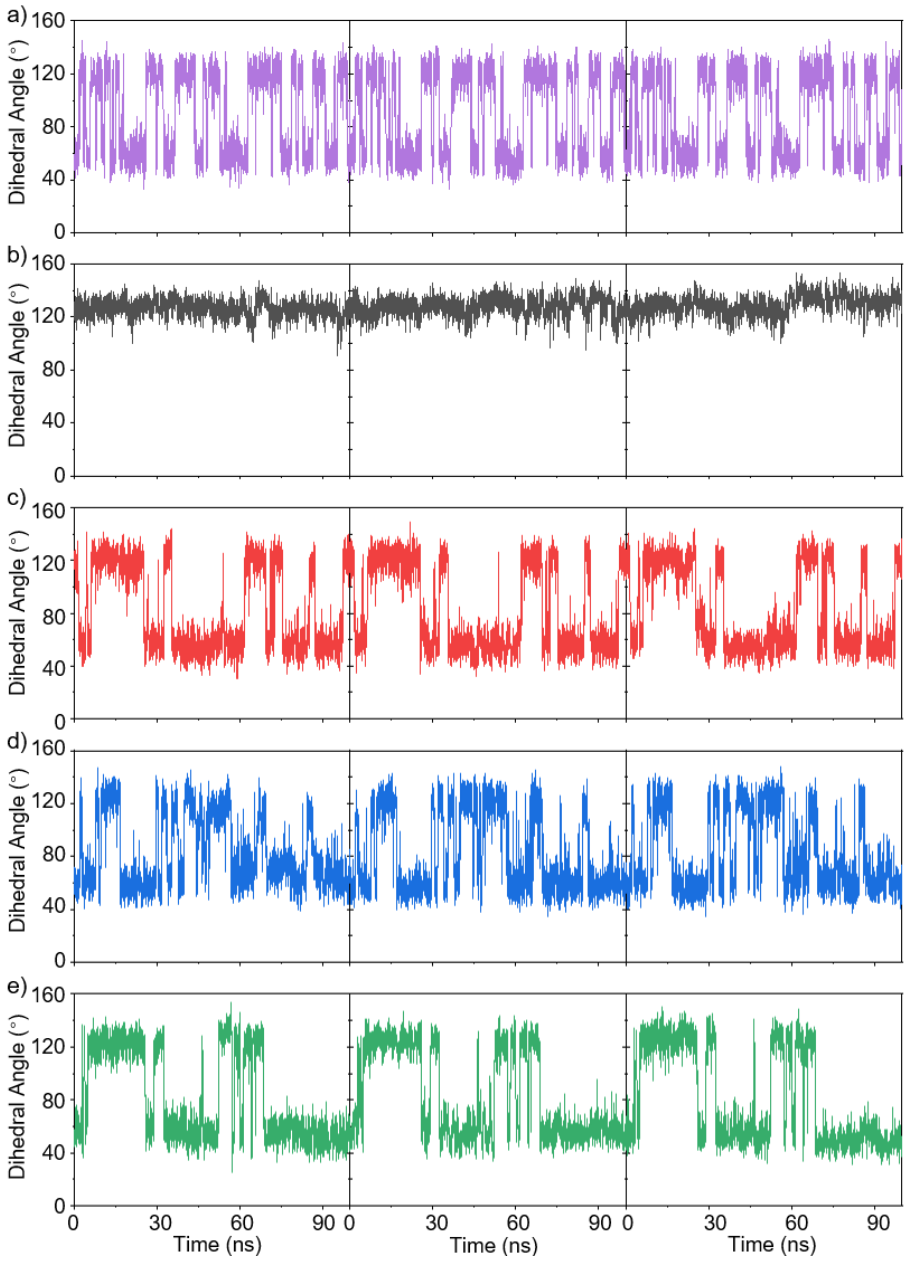

Figure S13. Three trajectories from molecular dynamics simulations of dihedral angles between a phenyl group plane and the ethylene plane in the TPE of $\mathbf{A_{TPE}S}$ (a), $\mathbf{R_{5F}}$ (b), $\mathbf{R'_{5F}}$ (c), $\mathbf{R_{5H}}$ (d), $\mathbf{R'_{5H}}$ (e).

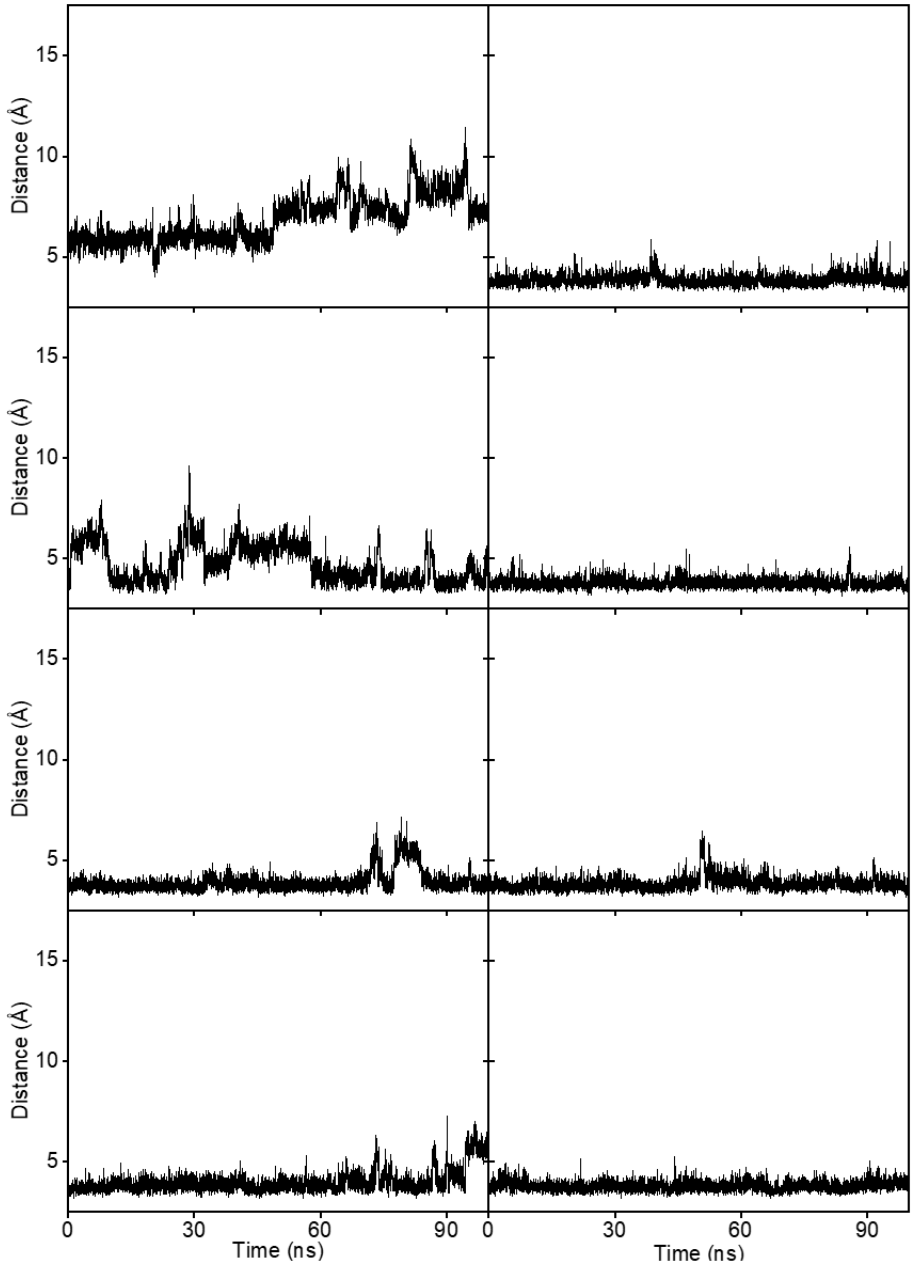

Figure S14. Two trajectories from molecular dynamics simulations of π-π distance between axle phenyl group III and wheel phenyl groups I, II in four branches of TPE in $\mathbf{R_{5F}}$ as shown in Figure 2a.

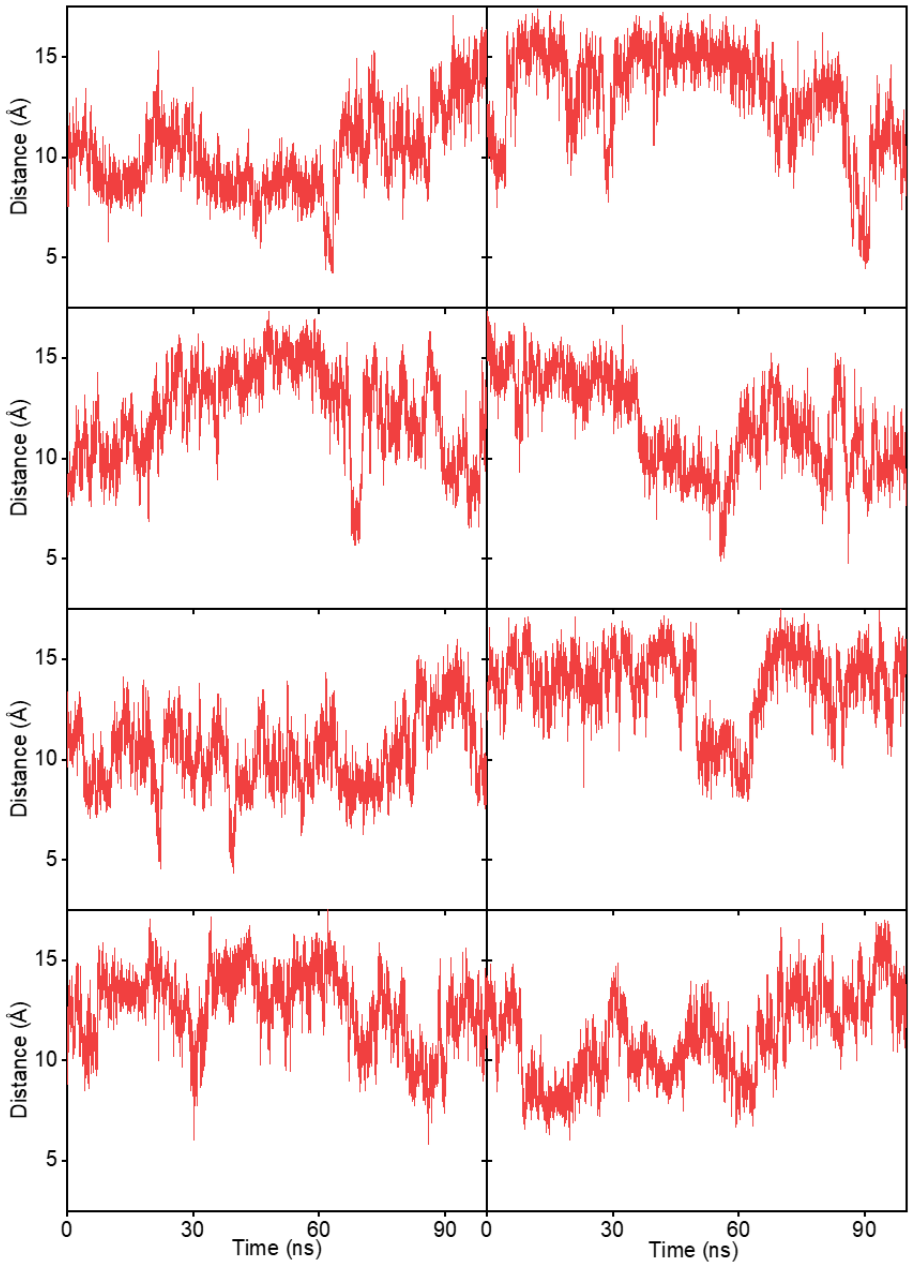

Figure S15. Two trajectories from molecular dynamics simulations of π-π distance between axle phenyl group III and wheel phenyl groups I, II in four branches of TPE in $\mathbf{R'_{5F}}$ as shown in Figure 2a.

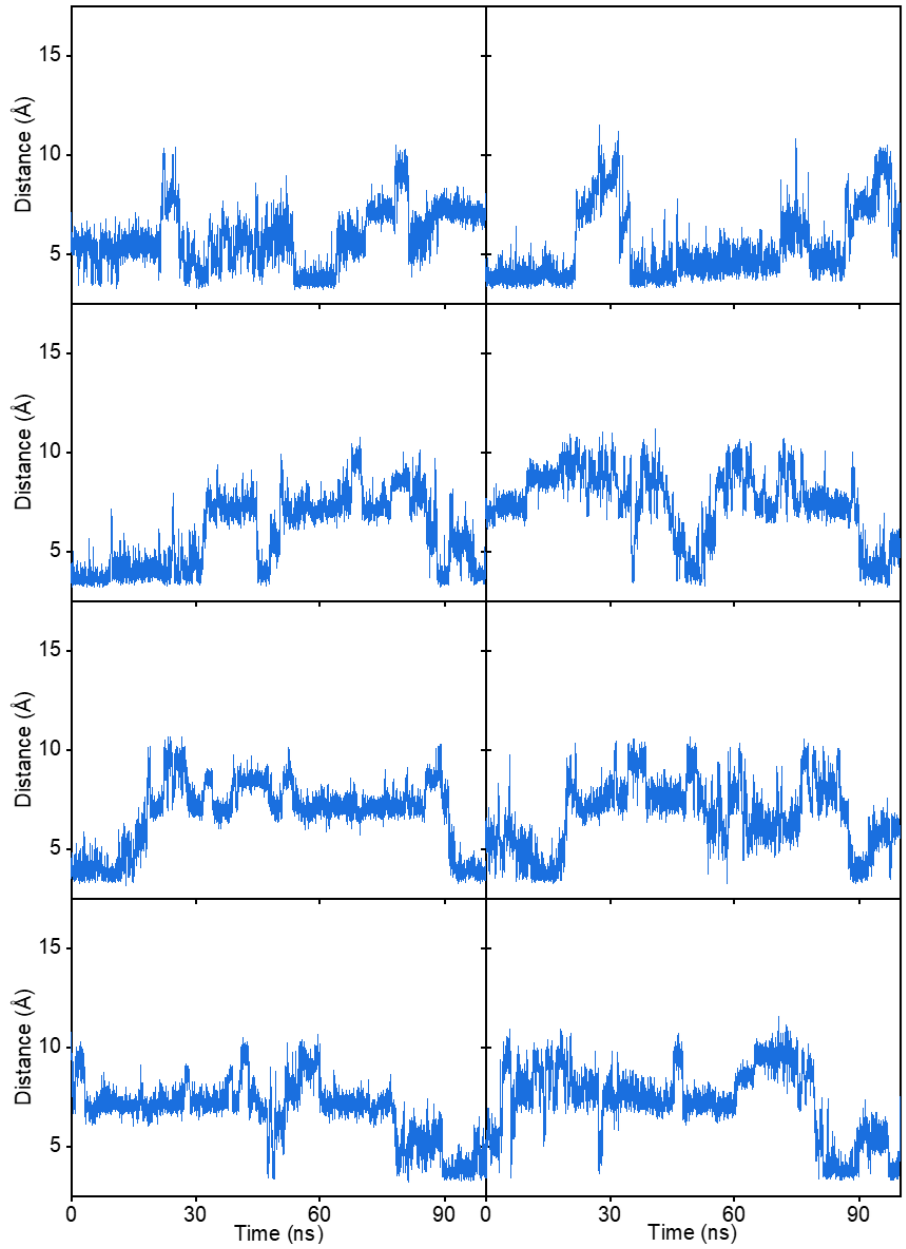

Figure S16. Two trajectories from molecular dynamics simulations of π-π distance between axle phenyl group III and wheel phenyl groups I, II in four branches of TPE in $\mathbf{R_{5H}}$ as shown in Figure 2a.

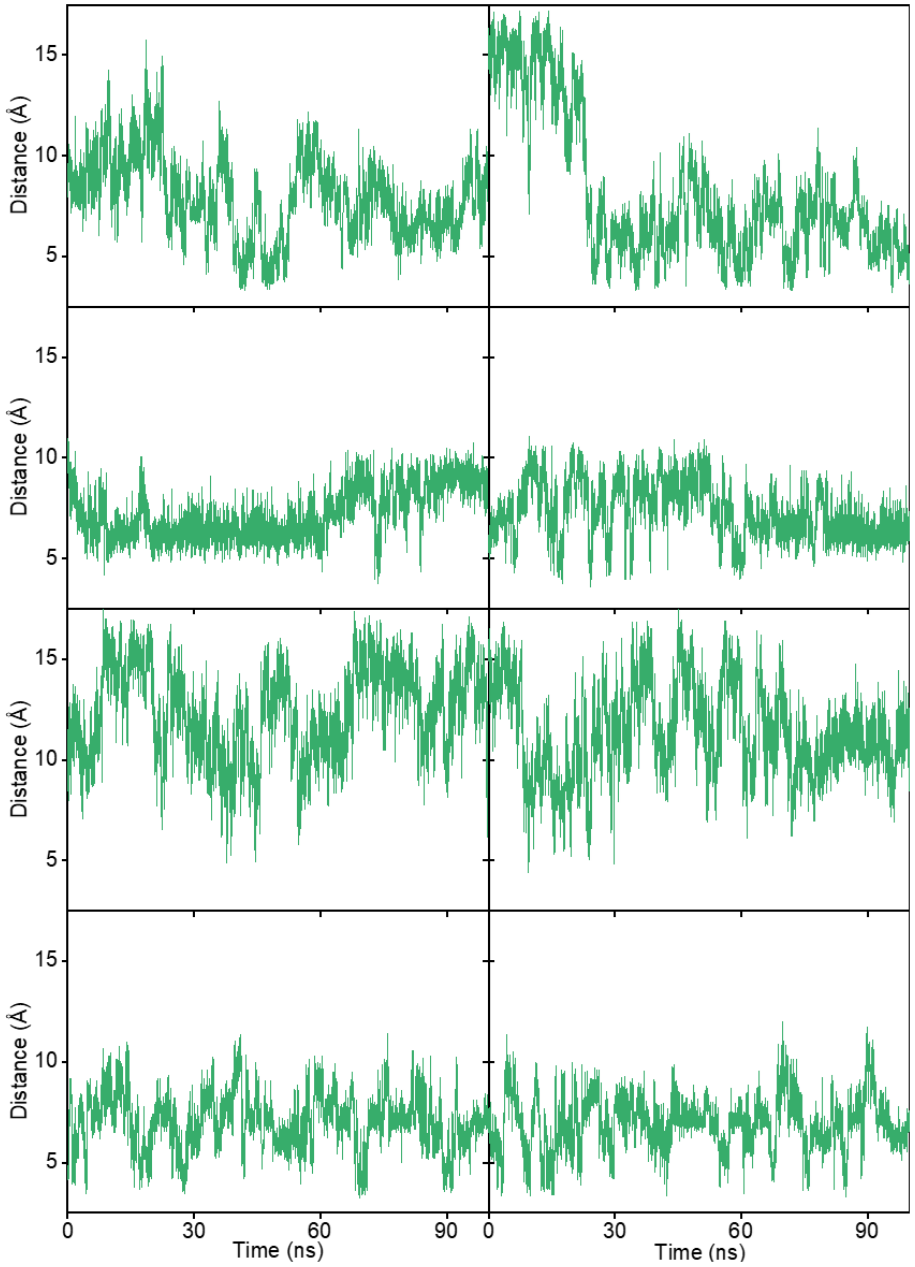

Figure S17. Two trajectories from molecular dynamics simulations of π-π distance between axle phenyl group III and wheel phenyl groups I, II in four branches of TPE in $\mathbf{R'_{5H}}$ as shown in Figure 2a.

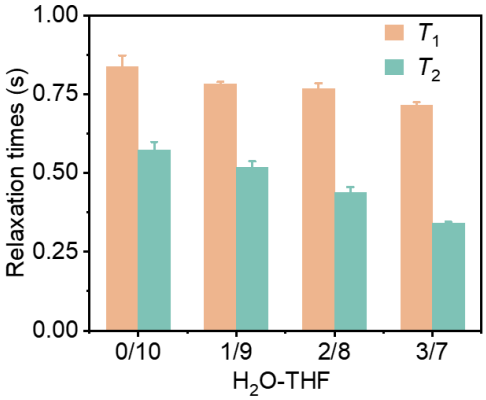

Figure S18. Relaxation times of wheel fluorines F_W at varying water content in **R_{5F}** THF solutions.

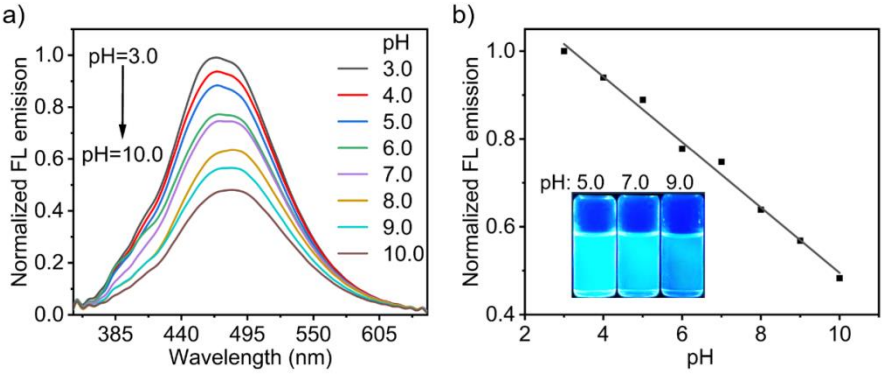

Figure S19. Normalized FL emission spectra (a) and the linear relationship between intensity and pH (b) in water-THF (3:7) solutions of **R_{5F}** at various pH values. Concentration: 25 μM.

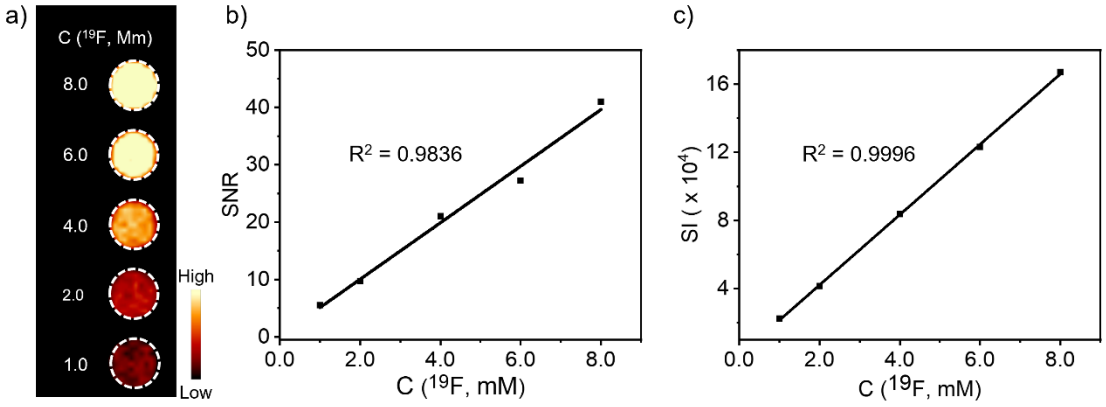

Figure S20. The ^{19}F MRI (a), and the linear correlation between SNR (b) and ^{19}F MRI SI (c) versus ^{19}F concentration of the nanoemusion **R_{5F}NPs.**

3. Preparation and Characterization of Compounds

3.1 Preparation and characterization of axle A_{TPE}

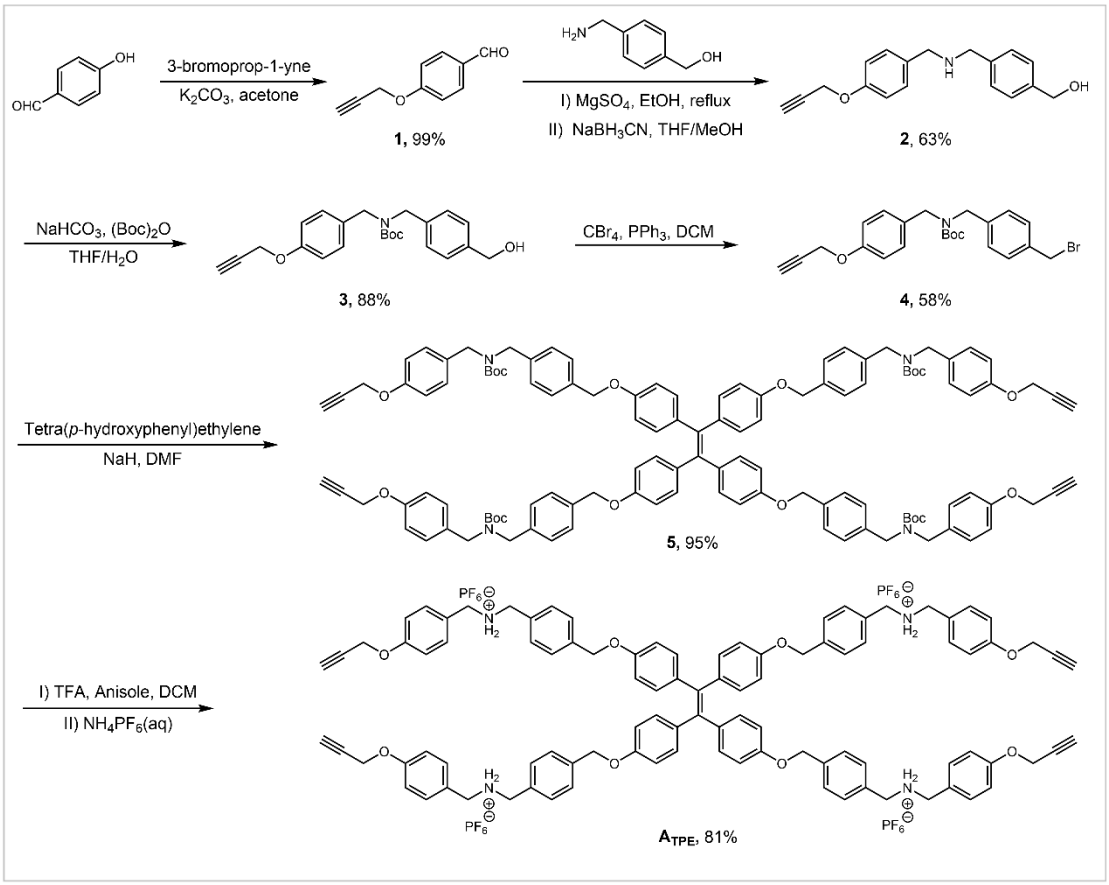

Figure S21. The synthetic route of axle $\mathbf{A_{TPE}}$.

4-(Prop-2-yn-1-yloxy)benzaldehyde (1)[1]**:** Following a previously reported procedure, a 500 mL round-bottom flask equipped with a magnetic stir bar was charged with 4-hydroxybenzaldehyde (10.00 g, 82.00 mmol), potassium carbonate (34.0 g, 246.0 mmol), propargyl bromide (21.2 mL, 246.0 mmol), and acetone (250 mL). The reaction mixture was refluxed for 4 hours, then allowed to cool to room temperature and quenched with water. The aqueous mixture was extracted twice with dichloromethane, and the combined organic layers were dried over anhydrous magnesium sulfate. The solvent was removed under reduced pressure, and the residue was purified by flash chromatography on silica gel using petroleum ether/ethyl acetate as the eluent to afford compound **1** as a pale yellow solid (13.00 g, 99% yield). **^{1}H NMR** (500 MHz, $CDCl_3$) δ 9.85 (s, 1H), 7.80 (d, J = 8.8 Hz, 2H), 7.04 (d, J = 8.8 Hz, 2H), 4.74 (d, J = 2.4 Hz, 2H), 2.57 (s, 1H). Spectral data were consistent with those reported previously.

(4-(((4-(Prop-2-yn-1-yloxy)benzyl)amino)methyl)phenyl)methanol (2): Under nitrogen atmosphere, (4-aminomethyl-phenyl)-methanol (4.12 g, 30.00 mmol) and anhydrous sodium sulfate (7.22 g, 60.00 mmol) were added to the solution of **1** (4.81 g, 30.00 mmol) in anhydrous ethanol (120 mL). The mixture was refluxed for 24 hours. Upon completion of the reaction, the solvent was evaporated under vacuum. Subsequently, the resulting residue was dissolved in a mixture of THF (60 mL) and MeOH (60 mL), followed by the gradual addition of $NaBH_3CN$ (7.54 g, 120.00 mmol) in portions at room temperature. The resulting mixture was allowed to continue stirred overnight before being quenched with a saturated NH_4Cl aqueous solution, concentrated under vacuum, and extracted with ethyl acetate (3 x 60 mL). Finally, the combined organic layer was dried over anhydrous sodium sulfate. After evaporation of ethyl acetate, the residue was purified by flash column chromatography on silica gel (DCM : MeOH = 10 : 1) to yield compound **2** as a yellow oil (5.3 g, 63% yield). **^{1}H NMR** (500 MHz, $CDCl_3$) δ 7.29 (s, 4H), 7.25 (d, *J* = 8.6 Hz, 2H), 6.94 (d, *J* = 8.6 Hz, 2H), 4.68 (d, *J* = 2.4 Hz, 2H), 4.63 (s, 2H), 3.76 (s, 2H), 3.73 (s, 2H), 2.60 (br, 2H), 2.52 (t, *J* = 2.4 Hz, 1H). **^{13}C NMR** (126 MHz, $CDCl_3$) δ 156.9, 140.1, 138.8, 132.5, 129.7, 128.6, 127.3, 115.0, 78.7, 75.7, 65.0, 56.0, 52.7, 52.4. **HRMS** (ESI^+) m/z: $[M+H]^+$ calculated for $C_{18}H_{20}NO_2^+$, 282.1489; found, 282.1490.

Tert-butyl (4-(hydroxymethyl)benzyl)(4-(prop-2-yn-1-yloxy)benzyl)carbamate (3): To a 100 mL three-neck flask, compound **2** (2.93 g, 10.41 mmol), sodium hydrogen carbonate (1.75 g, 20.82 mmol), THF (10 mL) and H_2O (10 mL) were added, and the mixture was stirred at room temperature for 10 minutes. Then, di-*tert*-butyl dicarbonate (3.27 g, 15.00 mmol) was added to this solution. The mixture was stirred at room temperature for 4 hours. After the white solid had been removed by filtration, the filtrate was collected and concentrated under a vacuum, followed by purification through flash column chromatography on silica gel (petroleum ether : ethyl acetate = 2:1), to give compound **3** as a colorless oil (3.51 g, 88% yield). **^{1}H NMR** (500 MHz, $CDCl_3$) δ 7.32 (d, *J* = 7.8 Hz, 2H), 7.20-7.13 (m, 4H), 6.93 (d, *J* = 8.7 Hz, 2H), 4.69-4.67 (m, 4H), 4.38-4.26 (m, 4H), 2.53 (t, *J* = 2.4 Hz, 1H), 1.96 (s, 1H), 1.49 (s, 9H). **^{13}C NMR** (126 MHz, $CDCl_3$) δ 156.8, 156.0, 140.0, 137.4, 131.0, 129.4, 128.8, 128.2, 127.6, 127.2, 115.0, 80.1, 78.6, 75.6, 65.1, 55.9, 48.6, 48.5, 28.5. **HRMS** (ESI^+) *m/z*: $[M+Na]^+$ calculated for $C_{23}H_{27}NO_4Na^+$, 404.1832; found, 404.1832.

Tert-butyl (4-(bromomethyl)benzyl)(4-(prop-2-yn-1-yloxy)benzyl)carbamate (4):

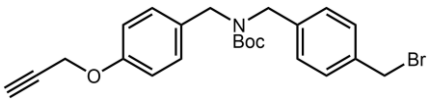

To a solution of compound **3** (3.51 g, 9.20 mmol) in DCM (30 mL), carbon tetrabromide (6.10 g, 18.40 mmol), and a solution of triphenylphosphine (4.83 g, 18.40 mmol) in DCM (10 mL) were added under nitrogen atmosphere. The mixture was stirred at room temperature for 4 hours. After removing the solvent, the residue was purified by silica gel chromatography (petroleum ether : ethyl acetate = 5:1), to afford compound **4** as a colorless oil (2.37 g, 58% yield). **^{1}H NMR** (500 MHz, $CDCl_3$) δ 7.35 (d, *J* = 7.9 Hz, 2H), 7.20-7.13 (m, 4H), 6.93 (d, *J* = 8.6 Hz, 2H), 4.69 (d, *J* = 2.4 Hz, 2H), 4.50 (s, 2H), 4.38-4.28 (m, 4H), 2.53 (t, *J* = 2.4 Hz, 1H), 1.49 (s, 9H). **^{13}C NMR** (126 MHz, $CDCl_3$) δ 156.9, 155.9, 138.6, 136.8, 130.9, 129.4, 129.3, 128.8, 128.4, 127.8, 115.0, 80.2, 78.6, 75.6, 55.9, 48.9, 48.6, 33.4, 28.5. **HRMS** (ESI^+) *m/z*: $[M+Na]^+$ calculated for $C_{23}H_{26}BrNO_3Na^+$, 466.0988; found, 466.0992.

Tetra-tert-butyl (((((ethene-1,1,2,2-tetrayltetrakis(benzene-4,1-diyl))tetrakis(oxy))tetrakis(methylene))tetrakis(benzene-4,1-diyl))tetrakis(methylene))tetrakis((4-(prop-2-yn-1-yloxy)benzyl)carbamate) (5):

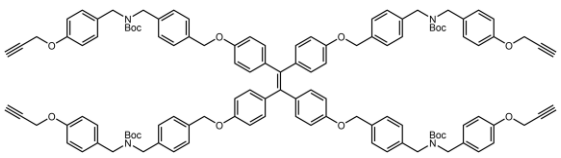

A suspension of sodium hydride (137.0 mg, 3.4 mmol, 60% in mineral oil) and tetrakis(4-hydroxyphenyl)ethylene (169.7 mg, 0.43 mmol) in 5 mL of *N*,*N*-dimethyl formaldehyde was stirred at 0°C for 30 minutes. Subsequently, a 15 mL solution of compound **4** (950.9 mg, 2.14 mmol) in *N*, *N*-dimethyl formaldehyde was slowly added to the suspension, and the resulting mixture was stirred at room temperature overnight. Following completion of the reaction as indicated by thin-layer chromatography (TLC), the reaction mixture was treated with water (150 mL) and then extracted twice with ethyl acetate (2 × 100 mL). The organic layers were combined, dried over anhydrous sodium sulfate, concentrated under vacuum, and purified by flash column chromatography on silica gel (petroleum ether : ethyl acetate = 1 : 1) to give compound **5** as a white wax (752.3 mg, 95% yield). **^{1}H NMR** (500 MHz, $CDCl_3$) δ 7.39 (d, *J* = 7.7 Hz, 8H), 7.26-7.16 (m, 16H), 6.98 (d, *J* = 8.2 Hz, 8H), 6.95 (d, *J* = 8.3 Hz, 8H), 6.76 (d, *J* = 8.3 Hz, 8H), 4.98 (s, 8H), 4.69 (d, *J* = 2.4 Hz, 8H), 4.42-4.29 (m, 16H), 2.53 (t, *J* = 2.4 Hz, 4H), 1.51 (s, 36H). **^{13}C NMR** (126 MHz, $CDCl_3$) δ 157.2, 157.0, 156.0, 138.6, 138.0, 137.2, 136.1, 132.7, 131.1, 129.5, 128.9, 128.3, 128.0, 127.7, 115.1,

114.0, 80.2, 78.7, 75.7, 69.8, 56.0, 49.0, 48.8, 48.6, 48.5, 28.6. **HRMS** (ESI^+) *m/z*: $[M+Na]^+$ calculated for $C_{118}H_{120}N_4O_{16}Na^+$, 1871.8592; found, 1871.8612.

A_{TPE}: At room temperature, trifluoroacetic acid (803.3 μL, 10.8 mmol) and anisole (587.0 μL, 5.4 mmol) were added to a solution of **5** (1.0 g, 0.54 mmol) in 10 mL dichloromethane, and the resulted mixture was stirred for 4 hours. Then, the reaction mixture was concentrated under a vacuum, followed by the addition of 10 mL of water and extraction with ethyl acetate (3 × 20 mL). The organic layers were combined, dried over anhydrous sodium sulfate, and concentrated under a vacuum, to yield a yellowish solid, which was directly utilized in the subsequent step without further purification. Subsequently, to a solution of the aforementioned product in 10 mL of acetone, 5 mL saturated NH_4PF_6 aqueous solution was added, and the resulting mixture was stirred for 5 h at room temperature. The reaction mixture was concentrated under vacuum, washed with water and diethyl ether, and then air-dried to afford compound **A_{TPE}** as a yellowish solid (888.0 mg, 81% yield). **^{1}H NMR** (500 MHz, DMSO-d_6) δ 7.50 (s, 16H), 7.43 (d, J = 8.4 Hz, 8H), 7.05 (d, J = 8.4 Hz, 8H), 6.89 (d, J = 8.4 Hz, 8H), 6.80 (d, J = 8.4 Hz, 8H), 5.02 (s, 8H), 4.83 (d, J = 2.4 Hz, 8H), 4.14 (s, 8H), 4.09 (s, 8H), 3.57 (t, J = 2.4 Hz, 4H). **^{13}C NMR** (126 MHz, DMSO-d_6) δ 157.6, 156.6, 138.1, 137.7, 136.5, 132.0, 131.4, 130.0, 128.1, 124.9, 115.0, 114.0, 79.1, 78.4, 68.8, 55.4, 49.8, 49.7. **HRMS** (ESI^+) *m/z*: $[M-4PF_6^-]^{4+}$ calculated for $C_{98}H_{92}N_4O_8^{4+}$, 363.1723; found, 363.1761.

3.2 Preparation and characterization of W_F and S

W_F and **S** were synthesized following our previous work and the corresponding references were cited.[2]

3.3 Preparation and characterization of $A_{TPE}S$

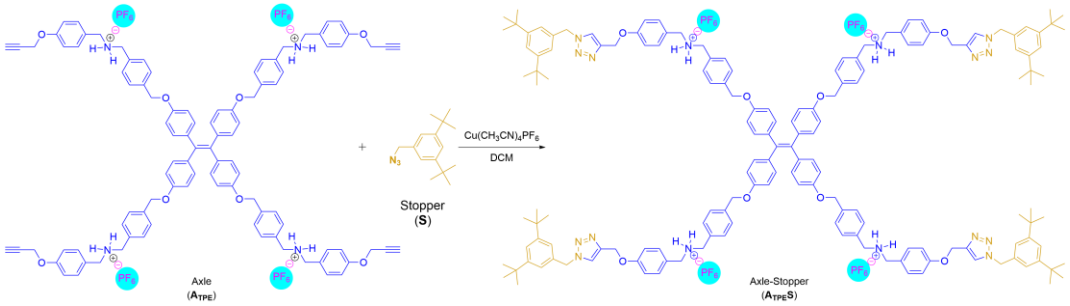

Procedure for synthesis of $A_{TPE}S$: Under an argon atmosphere, a mixture of $\mathbf{A_{TPE}}$ (200 mg, 0.098 mmol), stopper **S** (193 mg, 0.79 mmol), and $[Cu(CH_3CN)_4]PF_6$ (160.7 mg, 0.43 mmol) in dry dichloromethane was stirred for 12 hours. Upon completion of the reaction, the mixture was diluted with 100 mL dichloromethane, washed with water (3 × 100 mL), dried over anhydrous magnesium sulfate, and concentrated under vacuum. The residue was purified by flash column chromatography on silica gel (dichloromethane : methanol = 50 : 1) to give $\mathbf{A_{TPE}S}$ as a white wax (120.0 mg, 41% yield). **^{1}H NMR** (500 MHz, CD_3CN) δ 7.82 (s, 4H), 7.42 (t, J = 2.0 Hz, 4H), 7.32 (s, 16H), 7.22 (d, J = 8.4 Hz, 8H), 7.17 (d, J = 1.8 Hz, 8H), 6.91 (d, J = 8.4 Hz, 8H), 6.87 (d, J = 8.7 Hz, 8H), 6.69 (d, J = 8.7 Hz, 8H), 5.47 (s, 8H), 5.10 (s, 8H), 4.95 (s, 8H), 3.70 (s, 8H), 3.64 (s, 8H), 1.25 (s, 72H). **^{13}C NMR** (126 MHz, CD_3CN) δ 158.2, 158.1, 152.6, 144.8, 141.5, 139.8, 138.0, 136.8, 136.1, 134.1, 133.2, 130.4, 129.2, 128.7, 124.6, 123.5, 123.5, 115.5, 115.0, 70.4, 62.4, 55.0, 53.2, 53.0, 35.5, 31.6. **MALDI-TOF-MS** m/z: $[M–4PF_6^-–3H]^+$ calculated for $C_{158}H_{181}N_{16}O_8^+$, 2430.424; found, 2429.192.

3.4 Preparation and characterization of [5]rotaxanes R_{5F} and R_{5H}

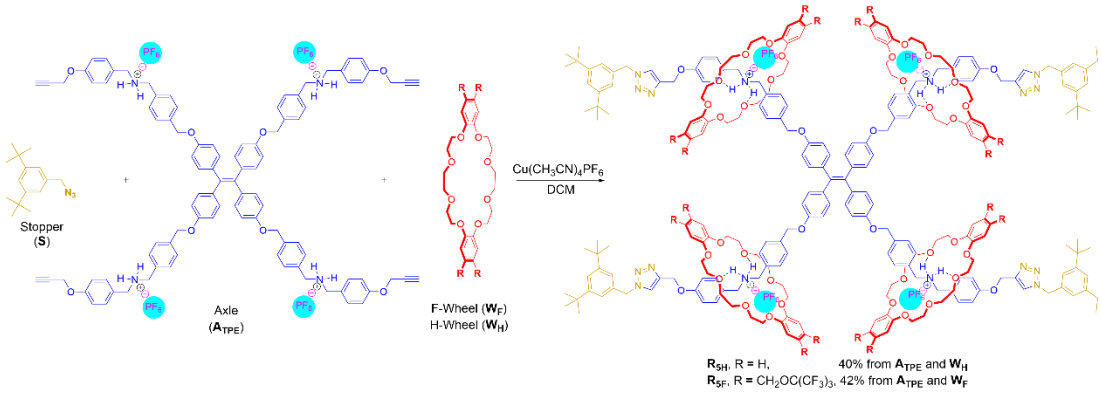

General procedure for the synthesis of [5]rotaxane R_{5F}: Under an argon atmosphere, a mixture of axle $\mathbf{A_{TPE}}$ (200 mg, 0.098 mmol) and F-Wheel $\mathbf{W_F}$ (850.1 mg, 0.59 mmol) in dry dichloromethane

was stirred at 45°C for 4 hours. Subsequently, stopper **S** (193.0 mg, 0.79 mmol) and $[Cu(CH_3CN)_4]PF_6$ (160.7 mg, 0.43 mmol) were added, and the resulting mixture was stirred for an additional 2 days. The reaction mixture was diluted with dichloromethane (100 mL), washed with water (3 × 100 mL), dried over anhydrous magnesium sulfate, and concentrated under a vacuum. The resulting residue was then purified by flash column chromatography on silica gel (dichloromethane : methanol = 50 : 1) to give $\mathbf{R_{5F}}$ as a white wax (361 mg, 42% yield). **^{1}H NMR** (500 MHz, CD_3CN) δ 7.85 (s, 4H), 7.45 (s, 4H), 7.45-7.42 (br, 8H), 7.37 (d, *J* = 8.4 Hz, 8H), 7.26 (d, *J* = 8.6 Hz, 8H), 7.22-7.21 (m, 8H), 7.04 (d, *J* = 8.4 Hz, 8H), 6.93 (d, *J* = 8.6 Hz, 8H), 6.86 (d, *J* = 8.7 Hz, 8H), 6.83 (s, 16H), 6.67 (d, *J* = 8.7 Hz, 8H), 5.51 (s, 8H), 5.10-5.05 (m, 32H), 5.01 (s, 8H), 4.76-4.69 (m, 16H), 4.64-4.62 (m, 8H), 4.11-4.04 (m, 32H), 3.84-3.75 (m, 32H), 3.69-3.63 (m, 32H), 1.28 (s, 72H). **^{19}F NMR** (471 MHz, CD_3CN) δ -71.33 (s, 144F), -73.28 (d, *J* = 706.7 Hz, 24F). **^{13}C NMR** (126 MHz, CD_3CN) δ 159.9, 158.1, 152.6, 148.9, 144.3, 139.7, 138.9, 138.3, 136.1, 133.3, 132.5, 132.0, 130.4, 127.9, 127.4, 125.4, 124.7, 123.6, 123.5, 121.4 (q, *J* = 293.3 Hz), 115.9, 115.0, 114.6, 81.3-80.1 (m), 71.8, 71.0, 70.0, 69.7, 69.2, 62.3, 55.1, 53.0, 52.9, 35.6, 31.6. **MALDI-TOF-MS** m/z: $[M–4PF_6^-–3H]^+$ calculated for $C_{334}H_{325}F_{144}N_{16}O_{56}^+$, 8191.078; found, 8192.009.

[5]rotaxane $\mathbf{R_{5H}}$: According to the general procedure for the synthesis of [5]rotaxane $\mathbf{R_{5F}}$, the

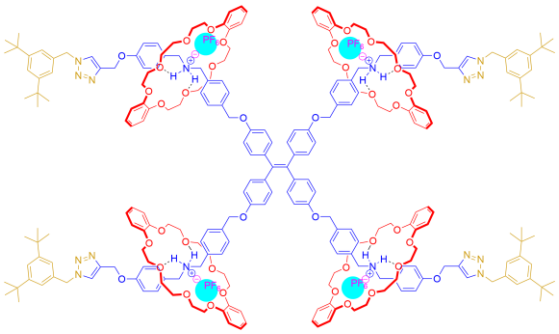

product $\mathbf{R_{5H}}$ was isolated by flash chromatography (dichloromethane : methanol = 50 : 1) as a white wax (192 mg, 40% yield). **^{1}H NMR** (500 MHz, CD_3CN) δ 7.88 (s, 4H), 7.45-7.41 (m, 12H), 7.32 (d, J = 7.9 Hz, 8H), 7.24-7.21 (m, 16H), 7.18 (d, J = 7.9 Hz, 8H), 6.91-6.89 (m, 8H), 6.83-6.79 (m, 16H), 6.77-6.72 (m, 24H), 6.70-6.67 (m, 8H), 5.51 (s, 8H), 5.01 (s, 8H), 4.86 (s, 8H), 4.67-4.65 (m, 8H), 4.57-4.56 (m, 8H), 4.03-4.00 (m, 32H), 3.73-3.71 (m, 32H), 3.56-3.49 (m, 32H), 1.28 (s, 72H). **^{19}F NMR** (471 MHz, CD_3CN) δ -73.32 (d, *J* = 707.1 Hz). **^{13}C NMR** (126 MHz, CD_3CN) δ 159.7, 158.0, 152.6, 149.6, 144.6, 139.9, 139.2, 138.0, 136.0, 133.1, 132.8, 131.9, 130.4, 128.4, 125.3, 124.8, 123.5, 123.5, 122.2, 115.6, 115.0, 113.4, 71.6, 71.1, 70.0, 68.8, 62.3, 55.1, 53.0, 52.9, 35.6, 31.6. **MALDI-TOF-MS** m/z: $[M–4PF_6–3H]^+$ calculated for $C_{254}H_{309}N_{16}O_{40}^+$, 4223.263; found, 4222.925.

3.5 Preparation and characterization of [5]rotaxanes R′$_{5F}$ and R′$_{5H}$

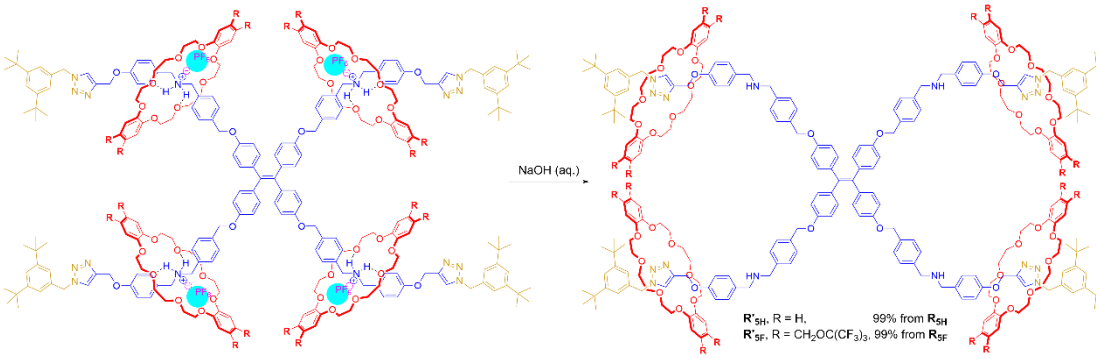

General procedure for the synthesis of [5]rotaxane R′$_{5F}$: **R$_{5F}$** (30.0 mg, 0.0034 mmol) was dissolved in 10 mL dichloromethane and washed with NaOH solution (1 M, 20 mL × 3). The resulting solution was dried with anhydrous magnesium sulfate and concentrated under vacuum to give **R′$_{5F}$** as a white wax (27.7 mg, 99% yield). **^{1}H NMR** (500 MHz, CD_3CN) δ 7.40 (t, *J* = 1.8 Hz, 4H), 7.29-7.25 (m, 8H), 7.22 (d, *J* = 7.7 Hz, 8H), 7.17-7.13 (m, 12H), 7.06-7.01 (m, 8H), 6.95 (s, 16H), 6.91-6.89 (m, 16H), 6.83 (d, *J* = 8.2 Hz, 8H), 5.38-5.33 (m, 16H), 5.11-5.05 (s, 40H), 4.04-4.02 (m, 32H), 3.65-3.58 (m, 48H), 3.13 (s, 32H), 1.23 (s, 72H). **^{19}F NMR** (471 MHz, CD_3CN) δ -71.30. **^{13}C NMR** (126 MHz, CD_3CN) δ 158.7, 158.3, 152.6, 152.4, 150.0, 146.0, 144.8, 141.6, 136.2, 136.1, 132.8, 129.8, 129.0, 128.4, 127.0, 125.5, 123.7, 123.4, 121.4 (q, *J* = 293.3 Hz), 115.7, 115.0, 82.0-79.4 (m), 70.3, 70.1, 69.5, 62.9, 54.9, 53.3, 53.1, 52.0, 35.5, 31.6. **MALDI-TOF-MS** m/z: $[M+H]^+$ calculated for $C_{334}H_{325}F_{144}N_{16}O_{56}^+$, 8191.078; found, 8191.861.

[5]rotaxane R′$_{5H}$: According to the general procedure for the synthesis of [5]rotaxane **R′$_{5F}$**, the

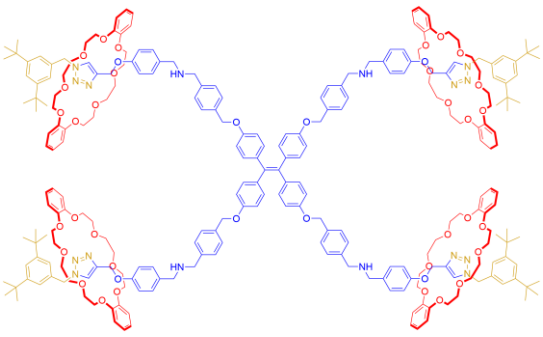

product **R′$_{5H}$** was isolated as a white wax (26 mg, 99% yield). **^{1}H NMR** (600 MHz, CD_3CN) δ 8.20 (s, 4H), 7.40 (s, 4H), 7.29 (s, 8H), 7.20 (s, 8H), 7.13 (s, 8H), 7.08-7.01 (m, 8H), 6.99-6.90 (m, 16H), 6.84 (m, 40H), 5.42 (s, 8H), 5.32 (s, 8H), 5.11 (s, 8H), 3.99-3.98 (m, 32H), 3.61-3.58 (m, 48H), 3.11 (s, 32H), 1.25 (s, 72H). **^{13}C NMR** (126 MHz, CD_3CN) δ 158.7, 152.4, 149.8, 149.3, 136.2, 132.9, 129.8, 129.0, 128.4, 123.4, 123.4, 122.3, 121.8, 115.8, 115.3, 113.2, 71.4, 70.4, 70.2, 69.5, 69.0, 55.3, 53.0, 35.5, 31.7. **MALDI-TOF-MS** m/z: $[M+H]^+$ calculated for $C_{254}H_{309}N_{16}O_{40}^+$, 4223.263; found, 4223.561.

4. Experiment Methods

4.1 Determination of molecular extinction coefficients

Compounds **R_{5F}**, **R'_{5F}**, **R_{5H}**, **R'_{5H}**, and **$A_{TPE}S$** were prepared at a range of concentrations in tetrahydrofuran (5, 10, 15, 20, 25 μM), and their UV absorbance was measured at 330 nm using a UV-Vis spectrophotometer (Shimadzu UV-2600). A linear relationship was then fitted between the absorbance and concentration, with the slope of the line representing the molar extinction coefficient.

4.2 Determination of T_1 and T_2

The pulse sequence for measuring T_1 was t1ir, T_1 of fluorine atoms (F_W) values were extracted from a series of GRE images with recovery times 0.2, 0.4, 0.8, 1.2, 2.2, 3.8, 5.4, 7.0 s, and 8 averages. The pulse sequence for measuring T_2 was cpmg, T_2 of fluorine atoms (F_W) values were extracted from a series of GRE images with recovery times 50, 100, 150, 250, 400, 600, 850, 1200 s, and 8 averages. T_1 of proton atoms (H_o) values were extracted from a series of GRE images with recovery times 0.2, 0.4, 0.8, 1.4, 2.4, 4.8, 8.0, 12.0 s, and 8 averages. The pulse sequence for measuring T_2 was cpmg, T_2 of proton atoms (H_o) values were extracted from a series of GRE images with recovery times 1800, 3300, 4800, 6400, 8200, 12800, 24000, 42000 s, and 8 averages. T_1 of proton atoms (H_m) values were extracted from a series of GRE images with recovery times 0.2, 0.4, 0.8, 1.2, 1.8, 3, 6.4, 8.8 s, and 8 averages. T_2 of proton atoms (H_m) values were extracted from a series of GRE images with recovery times 210, 880, 1560, 2580, 3800, 6600, 9600, 12800 s, and 8 averages.

4.3 ^{19}F MRI phantom experiments of W_F, R_{5F}, and R'_{5F}.

^{19}F MRI phantom experiments were performed on a Bruker BioSpec 400 MHz MRI system. The temperature of the magnet room was maintained at 30 °C during the experiment. The ^{19}F phantom images were acquired using a RARE pulse sequence, RARE factor = 4, matrix size = 32 × 32, slice thickness = 20 mm, FOV = 3.0 cm × 3.0 cm, TR = 600 ms, TE = 17.5 ms, scan time = 307 s. The responsive ^{19}F MRI phantom experiments were performed using the following parameters: RARE factor = 4, matrix size = 32 × 32, slice thickness = 20 mm, FOV = 3.0 cm × 3.0 cm, TR = 800 ms, TE = 3.0 ms, scan time = 409 s.

4.4 R_{5F}, R'_{5F}, Rx-2 and Rx-2′-absorbed PTFE microparticles experiments

According to the reported literature,[3] 20 mg of each **R_{5F}**, **R'_{5F}**, **Rx-2**, **and Rx-2′** were coated on PTFE powder (200 mg, 200 μm particle size) respectively followed by adding a solvent mixture of acetone/H_2O (6:4, v:v, 400 μL). The resulting mixtures were stirred at room temperature for 20 min and filtrated through a sand core funnel. Finally, the absorbed PTFE powder was freeze-dried by a vacuum freeze-dryer and reserved for use.

4.5 Preparation of R_{5F} nanoparticles (R_{5F}NPs)

R_{5F} (0.5 mg), lecithin (8.0 mg), DSPE-PEG_{2000} (1.0 mg), and tricaproin (30.0 mg) were co-dissolved in 0.6 mL of chloroform. The solvent was subsequently evaporated under reduced pressure to form a thin lipid film. The resulting film was hydrated with 1 mL of water and subjected to sonication for 15 minutes to generate the nanoemusion **R_{5F}NPs**. The prepared **R_{5F}NPs** were stored at 4 °C for further use. (Note: Before formulation, **R_{5F}** was paired with a bulky counterion, sodiumtetrakis(pentafluorophenyl)borate.)

4.6 Animals and tumor model

The U87-MG tumor model was established by subcutaneously injecting U87-MG cells (1×10^7) suspended in 0.1 mL of PBS on the flank of the female BALB/c nude mouse.

4.7 *In vitro* ^{19}F MRI of the nanoemusion R_{5F}NPs

The nanoemusion **R_{5F}NPs** was serially diluted with water to give a series of ^{19}F concentrations: 8, 6, 4, 2, and 1 mM, respectively. The ^{19}F MRI phantom experiments were performed on a 9.4T Bruker BioSpec MRI system at 25 ^{o}C using a RARE sequence (matrix size = 32 × 32, FOV = 30 mm × 30 mm, slice thickness = 20 mm, TR = 1500 ms, TE = 3.00 ms, RARE factor = 4, 64 averages, scan time = 768 ms).

4.8 *In vivo* ^{19}F MRI of the nanoemusion R_{5F}NPs

The mice had free access to water and food until tumor size reached approximately 150 mm^3. The tumor-bearing mice were intratumorally injected 0.1 mL of nanoemusion **R_{5F}NPs** (C_F = 40

mM). ^{19}F MRI was performed on 9.4T Bruker BioSpec MRI system. ^{1}H T_2-weighed MRI scan using a RARE sequence (TR = 2500 ms, TE = 33 ms, FOV = 30 mm × 30 mm, slice thickness = 1 mm, RARE factor = 8, matrix size = 256 × 256, 10 averages). ^{19}F MRI was performed through a RARE sequence (TR = 3000 ms, TE = 3 ms, FOV = 30 mm × 30 mm, slice thickness = 15 mm, matrix size = 32 × 32, 128 averages, scan time = 1h48min).

4.9 MD simulations

The initial systems for MD simulations were built by placing the rotaxanes and $\mathbf{A_{TPE}S}$ in the center of a cubic box with a volume of 80×80×80 Å^3 containing 6000 acetonitrile molecules. Here, the configuration of fluorinated wheels in $\mathbf{R_{5F}}$ was adopted from X-ray structure published in our previous study,[2] and the wheels in $\mathbf{R'_{5F}}$ and $\mathbf{R'_{5H}}$ were truncated from the PFBM groups from the experimental structure. The $\mathbf{A_{TPE}S}$ and its protonated configurations (axle conformation) were generated by quantum chemical calculations with PM6 method performed on Gaussian09 software[4]. All the modeling systems were built by PyMol and PackMol program.[5] Then, MD simulations were performed by AMBER18 software package supported GPU computation with the CUDA version of pmemd program.[6] The topology parameters of the modeling systems were generated by quantum mechanical HF/6-31G* optimizations from Gaussian09 software[4] cooperated with RESP[7] approach and GAFF[8] force field from AMBER package.

Each of the modeling systems was carried out 500 ns MD simulations with conventional steps of minimization and equilibration in advance. During the equilibration processes, the systems were heated in constant volume (NVT ensemble) and equilibrated in constant pressure (NPT ensemble) conditions. After 10 ns of equilibration, the production MD simulations were performed under the constant pressure of 1.0 bar using Berendsen barostat at 300 K. The time step was set to 1 fs and every 10 ps saved one snapshot. Only the final 100 ns of simulated trajectories were used for analyses which were applied CPPTRAJ program[9] and in-house scripts.

4.10 Statistical analysis

The analyzed data are presented as mean ± standard deviation of n = 3 replicates. Statistical significance was assessed by unpaired two-tailed Student's t-test. Asterisks indicate significant differences: $p < 0.05$ was considered the probability threshold for statistical significance, *$p < 0.05$, **$p < 0.01$, ***$p < 0.001$.

5. References

(1) Giguère, J.-B.; Thibeault, D.; Cronier, F.; Marois, J.-S.; Auger, M.; Morin, J.-F. Synthesis of [2]- and [3]Rotaxanes through Sonogashira Coupling. *Tetrahedron Lett.* **2009**, *50*, 5497-5500.

(2) Yang, L.; Li, Y.; Jiang, M.; Zhou, R.; Cong, H.; Yang, M.; Zhang, L.; Li, S.; Yang, Y.; Liu, M.; Zhou, X.; Jiang, Z.-X.; Chen, S. Fluorinated Rotaxanes as Sensitive ^{19}F MRI Agents: Threading for Higher Sensitivity. *Chin. Chem. Lett.* **2024**, *35*, 109512.

(3) Cai, L.; Chen, Q.; Guo, J.; Liang, Z.; Fu, D.; Meng, L.; Zeng, J.; Wan, Q. Recyclable Fluorous-Tag Assisted Two-Directional Oligosaccharide Synthesis enabled by Interrupted Pummerer Reaction Mediated Glycosylation. *Chem. Sci.* **2022**, *13*, 8759-8765.

(4) Frisch, M. J.; Trucks, G. W.; Schlegel, H. B.; Scuseria, G. E.; Robb, M. A.; Cheeseman, J. R.; Scalmani, G.; Barone, V.; Mennucci, B.; Petersson, G. A.; Nakatsuji, H.; Caricato, M.; Li, X.; Hratchian, H. P.; Izmaylov, A. F.; Bloino, J.; Zheng, G.; Sonnenberg, J. L.; Hada, M.; Ehara, M.; Toyota, K.; Fukuda, R.; Hasegawa, J.; Ishida, M.; Nakajima, T.; Honda, Y.; Kitao, O.; Nakai, H.; Vreven, T.; Montgomery, J. A.; Jr.; Peralta, J. E.; Ogliaro, F.; Bearpark, M.; Heyd, J. J.; Brothers, E.; Kudin, K. N.; Staroverov, V. N.; Kobayashi, R.; Normand, J.; Raghavachari, K.; Rendell, A.; Burant, J. C.; Iyengar, S. S.; Tomasi, J.; Cossi, M.; Rega, N.; Millam, J. M.; Klene, M.; Knox, J. E.; Cross, J. B.; Bakken, V.; Adamo, C.; Jaramillo, J.; Gomperts, R.; Stratmann, R. E.; Yazyev, O.; Austin, A. J.; Cammi, R.; Pomelli, C.; Ochterski, J. W.; Martin, R. L.; Morokuma, K.; Zakrzewski, V. G.; Voth, G. A.; Salvador, P.; Dannenberg, J. J.; Dapprich, S.; Daniels, A. D.; Farkas, Ö.; Foresman, J. B.; Ortiz, J. V.; Cioslowski, J.; Fox, D. J. Gaussian 09, Revision A.1; Gaussian, Inc.: Wallingford, CT, **2009**.

(5) Martínez, L.; Andrade, R.; Birgin, E. G.; Martínez, J. M., PACKMOL: A Package for Building Initial Configurations for Molecular Dynamics Simulations. *J. Comput. Chem.* **2009,** *30*, 2157-2164.

(6) Salomon-Ferrer, R.; Götz, A. W.; Poole, D.; Le Grand, S.; Walker, R. C. Routine Microsecond Molecular Dynamics Simulations with AMBER on GPUs. 2. Explicit Solvent Particle Mesh Ewald. *J. Chem. Theory Comput.* **2013,** *9*, 3878-3888.

(7) Bayly, C. I.; Cieplak, P.; Cornell, W.; Kollman, P. A. A Well-Behaved Electrostatic Potential Based Method using Charge Restraints for Deriving Atomic Charges: The RESP Model. *J. Phys. Chem.* **1993,** *97*, 10269-10280.

(8) Wang, J.; Wolf, R. M.; Caldwell, J. W.; Kollman, P. A.; Case, D. A. Development and Testing of A General Amber Force Field. *J. Comput. Chem.* **2004,** *25*, 1157-1174.

(9) Roe, D. R.; Cheatham, T. E. III. PTRAJ and CPPTRAJ: Software for Processing and Analysis of Molecular Dynamics Trajectory Data. *J. Chem. Theory Comput.* **2013,** *9*, 3084-3095.

6. NMR Spectra and HRMS Spectra of Compounds

Compound 1: ^{1}H NMR (500 MHz, $CDCl_3$)

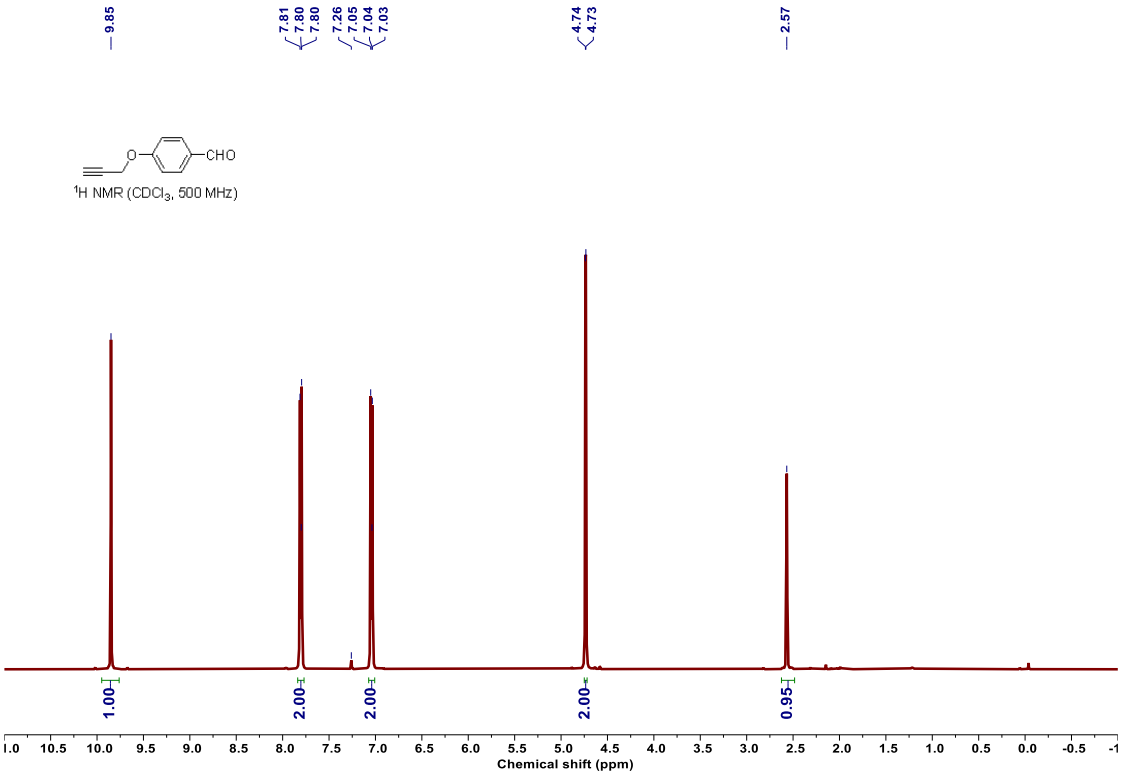

Compound 2: ^{1}H NMR (500 MHz, $CDCl_3$)

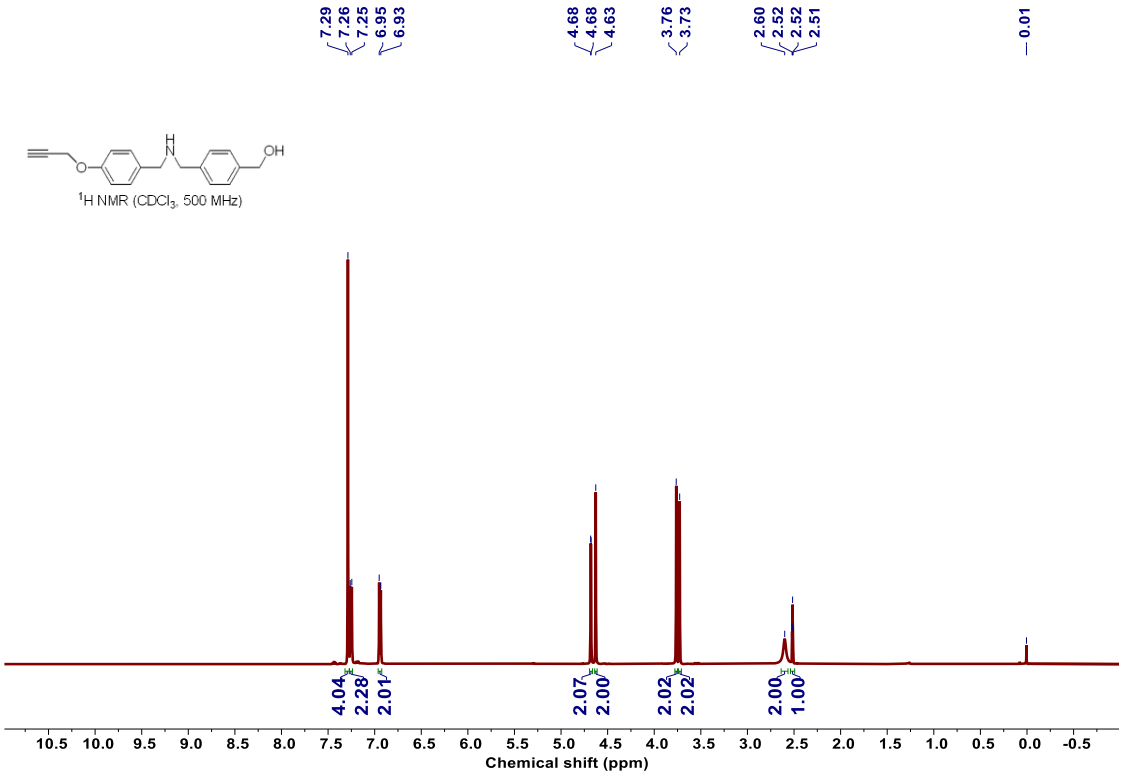

Compound 2: ^{13}C NMR (126 MHz, $CDCl_3$)

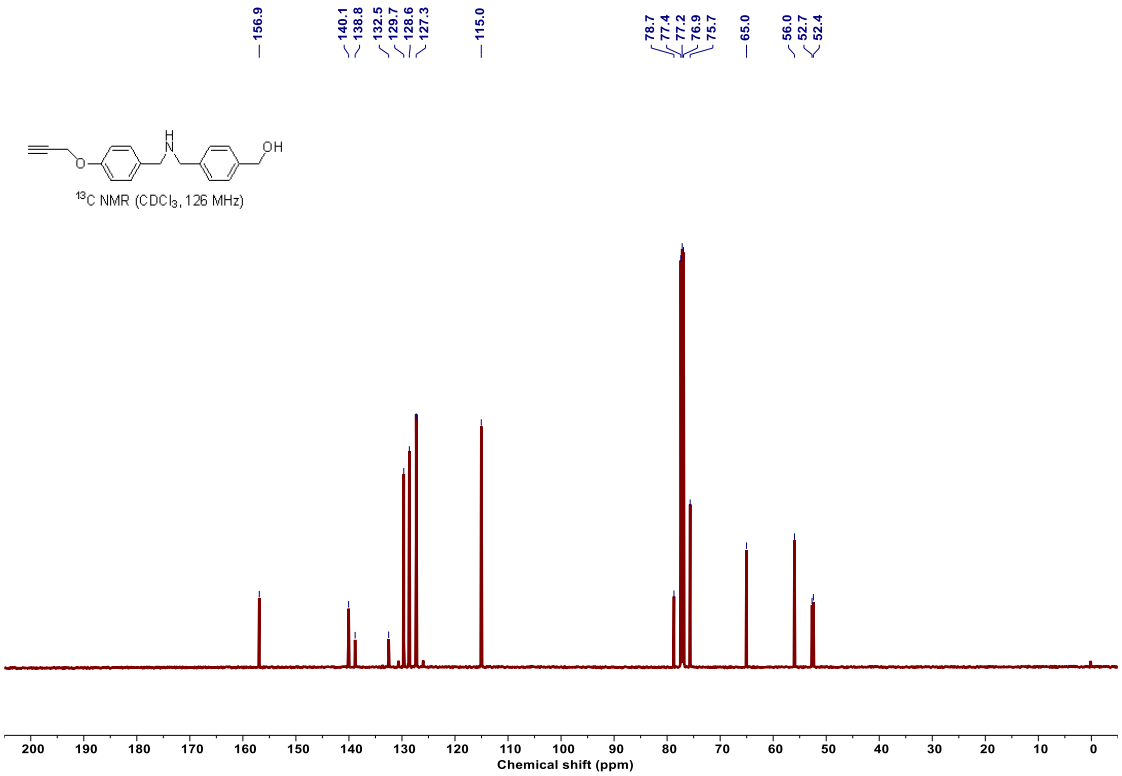

Compound 2: HRMS (ESI, $[M+H]^+$)

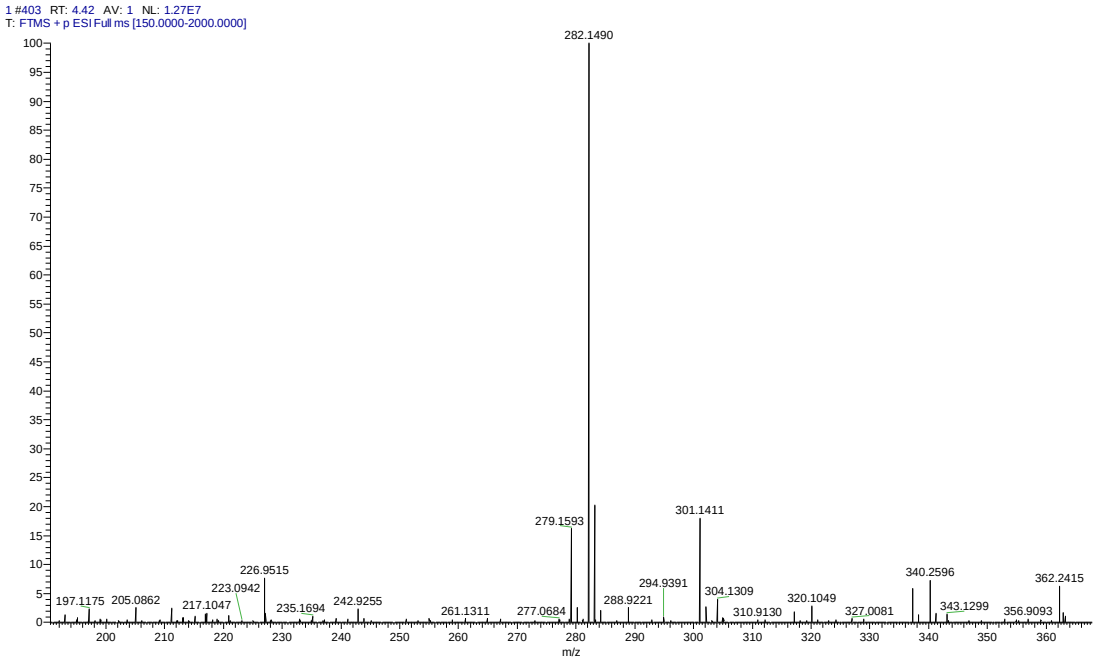

Compound 3: ^{1}H NMR (500 MHz, $CDCl_3$)

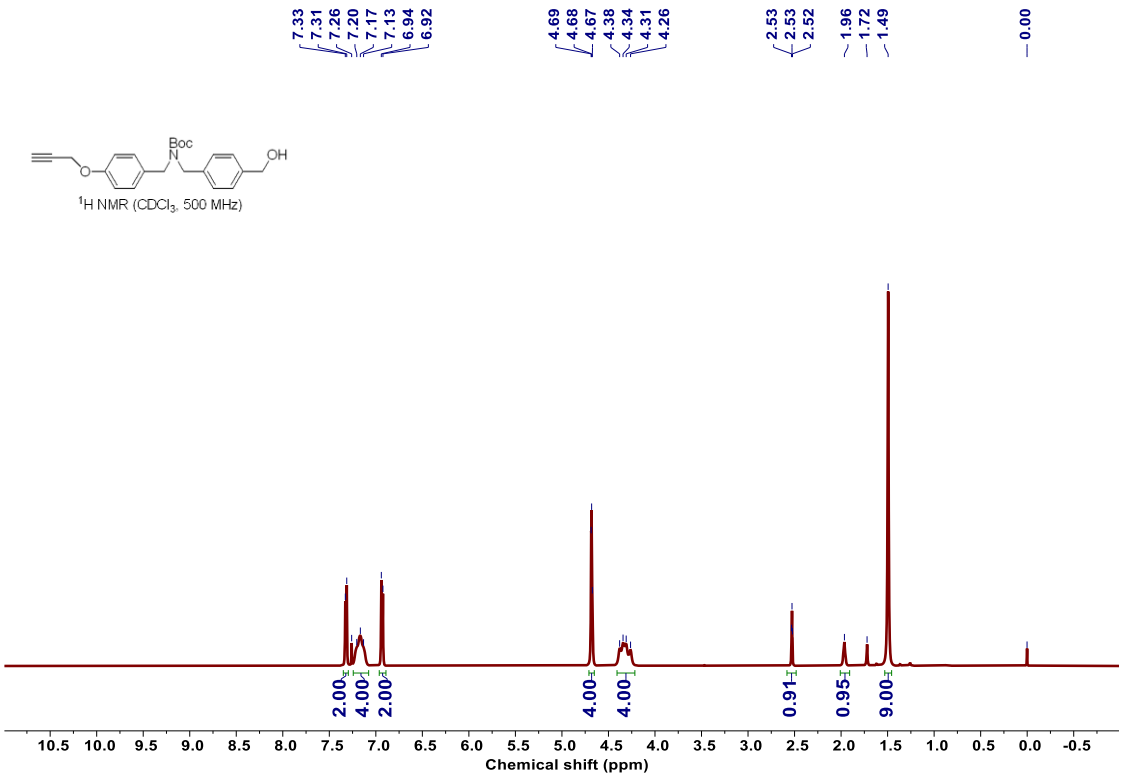

Compound 3: ^{13}C NMR (126 MHz, $CDCl_3$)

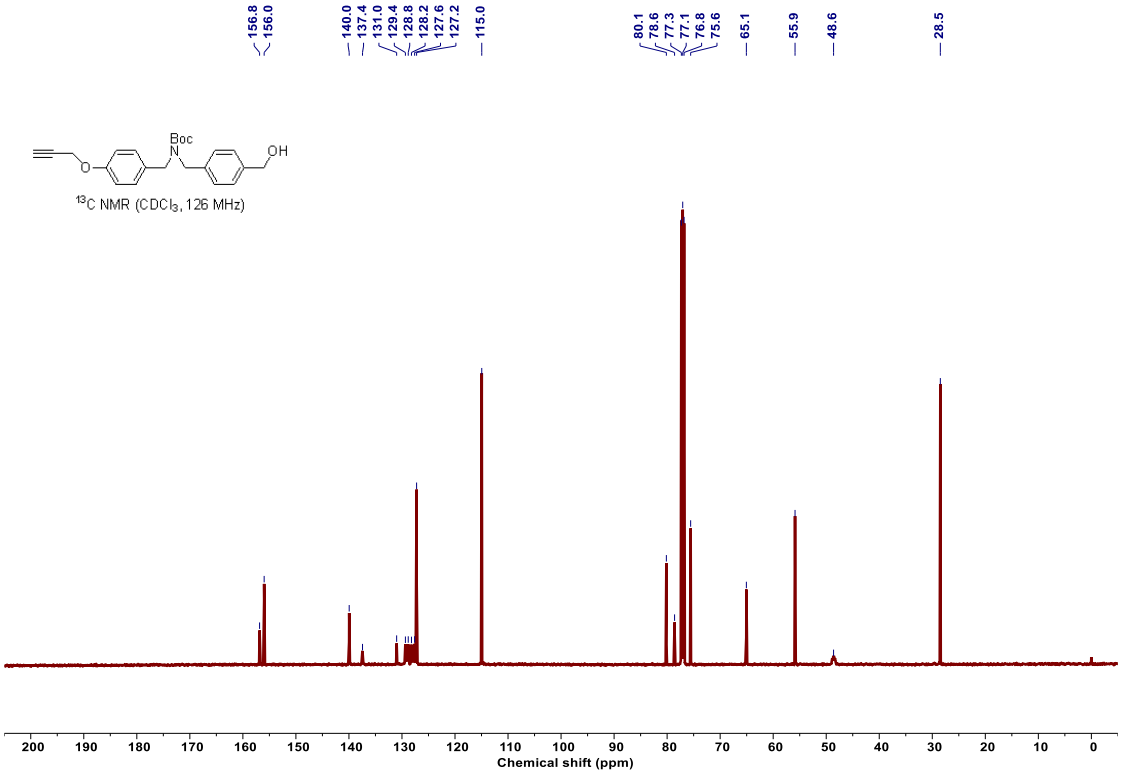

Compound 3: HRMS (ESI, $[M+Na]^+$)

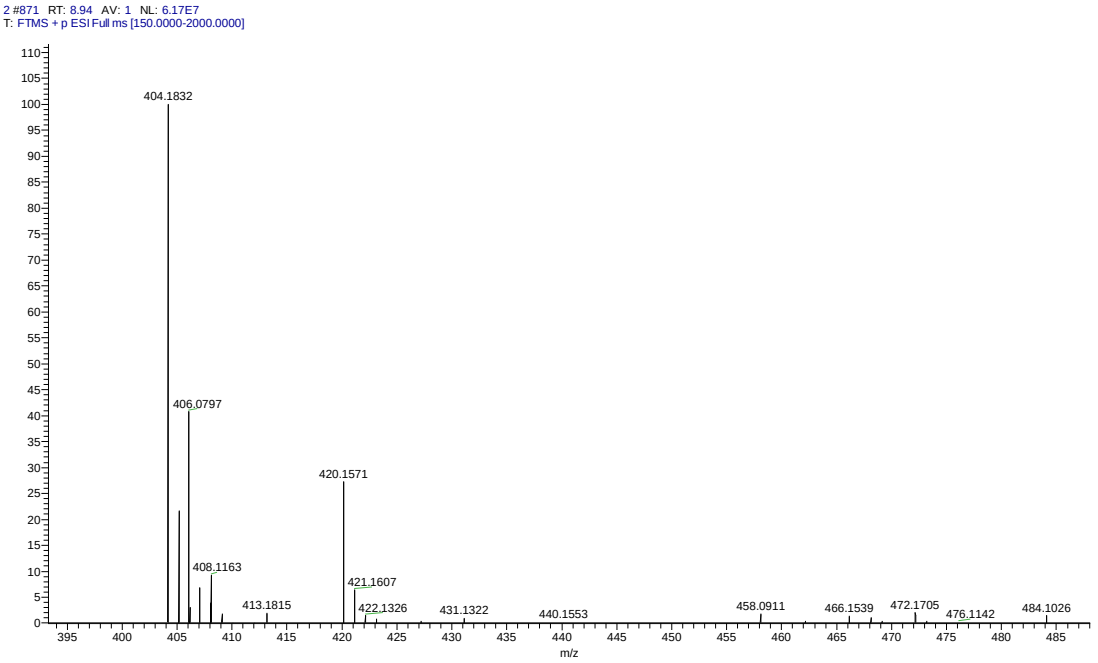

Compound 4: ^1H NMR (500 MHz, $CDCl_3$)

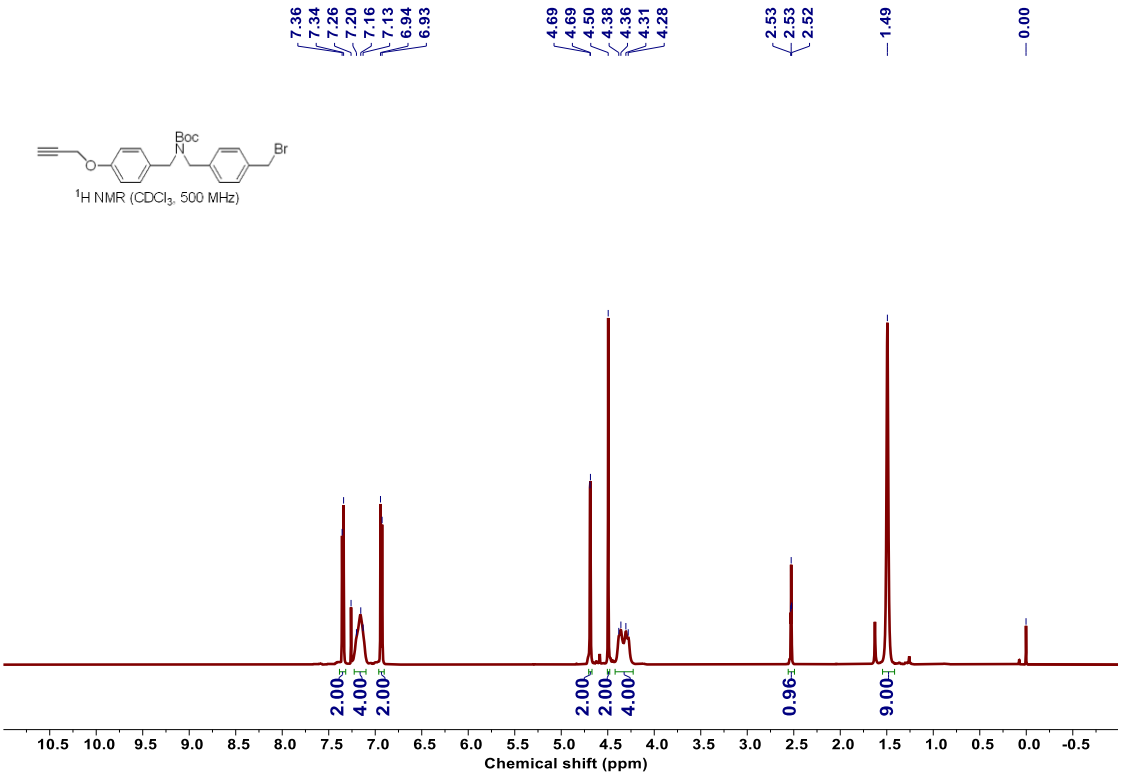

Compound 4: ^{13}C NMR (126 MHz, $CDCl_3$)

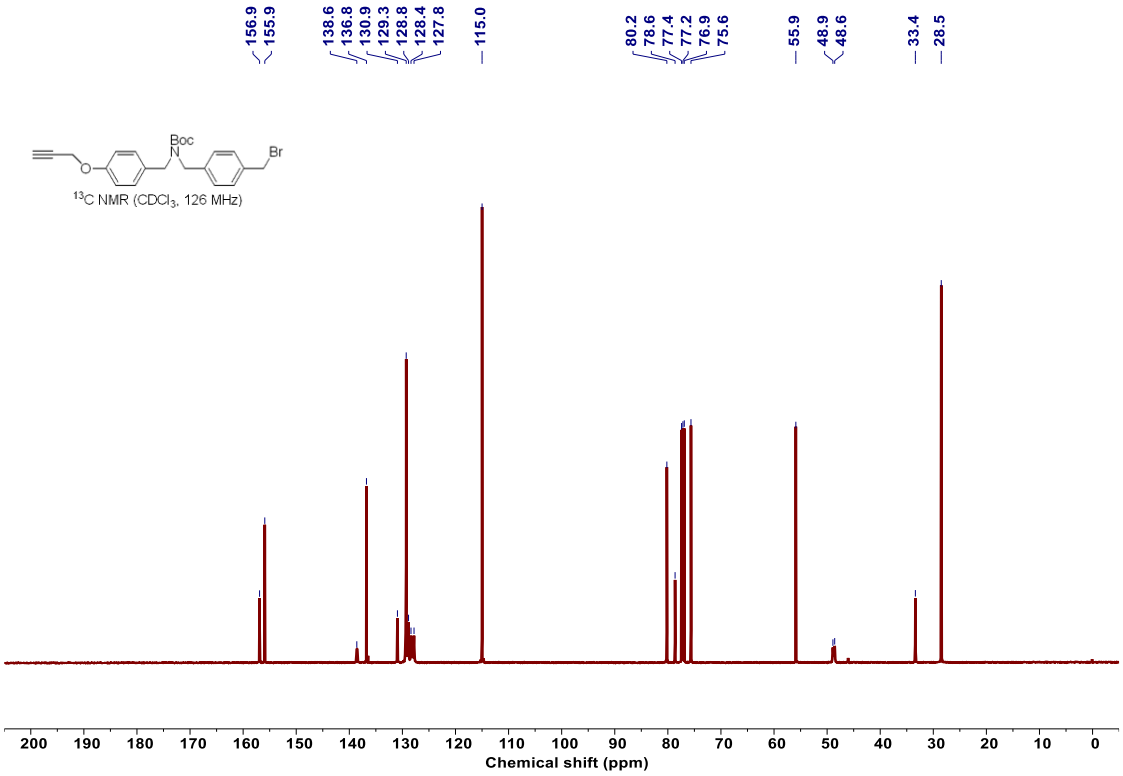

Compound 4: HRMS (ESI, $[M+Na]^+$)

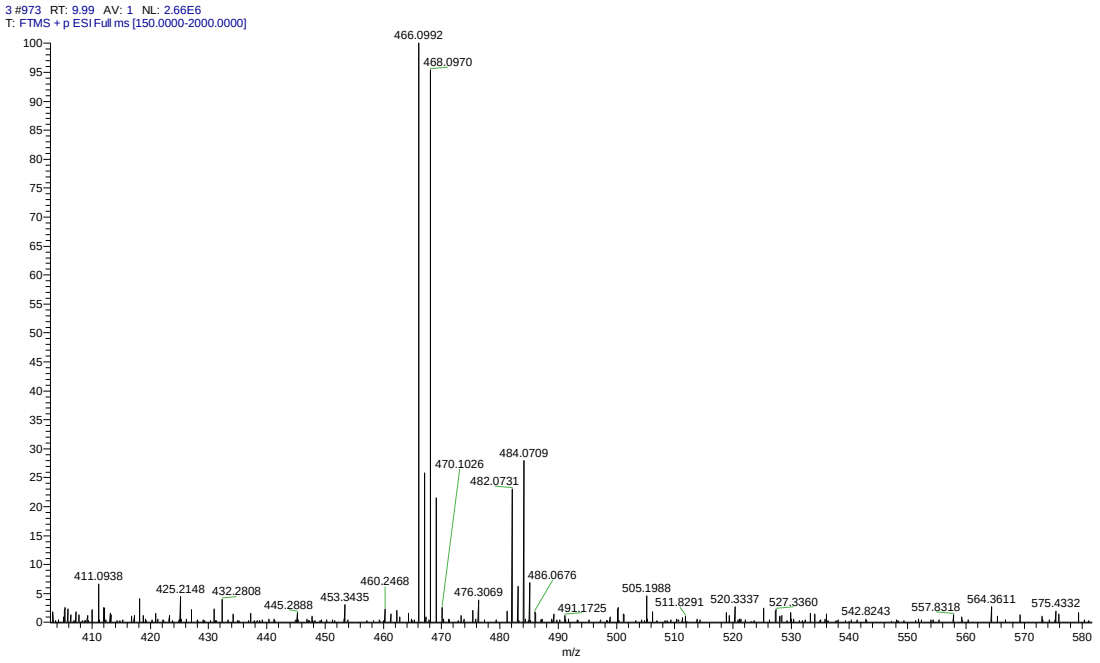

Compound 5: ^{1}H NMR (500 MHz, $CDCl_3$)

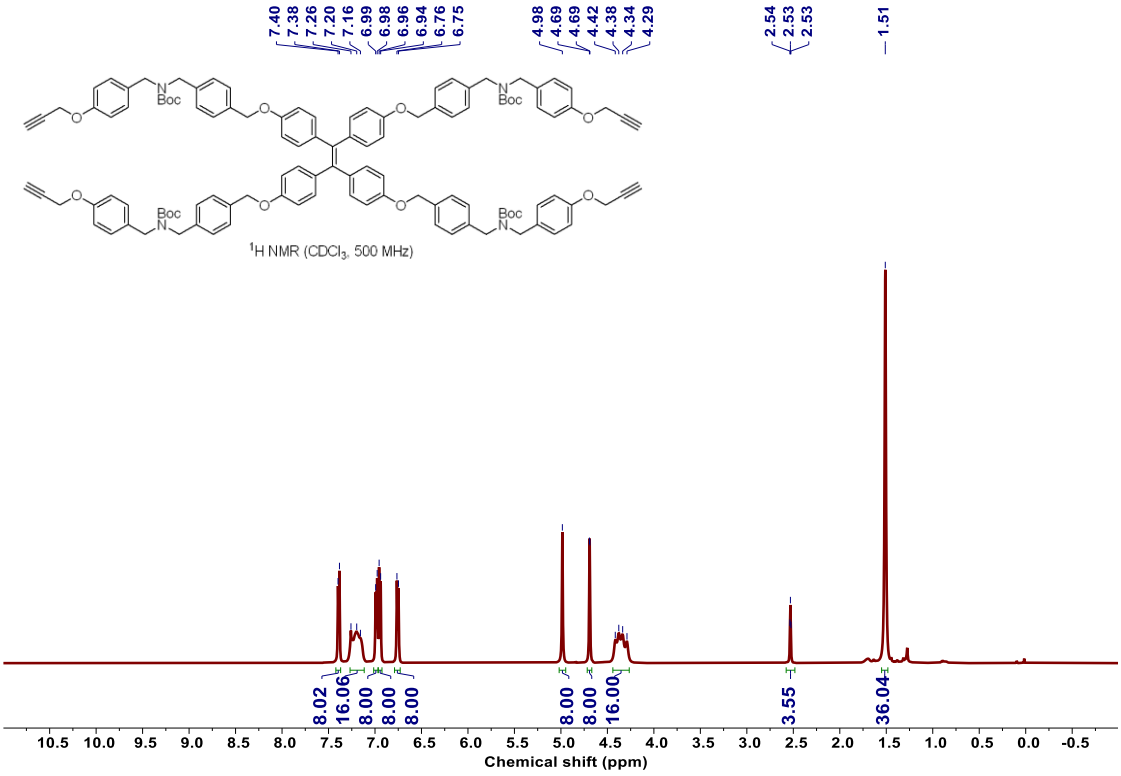

Compound 5: ^{13}C NMR (126 MHz, $CDCl_3$)

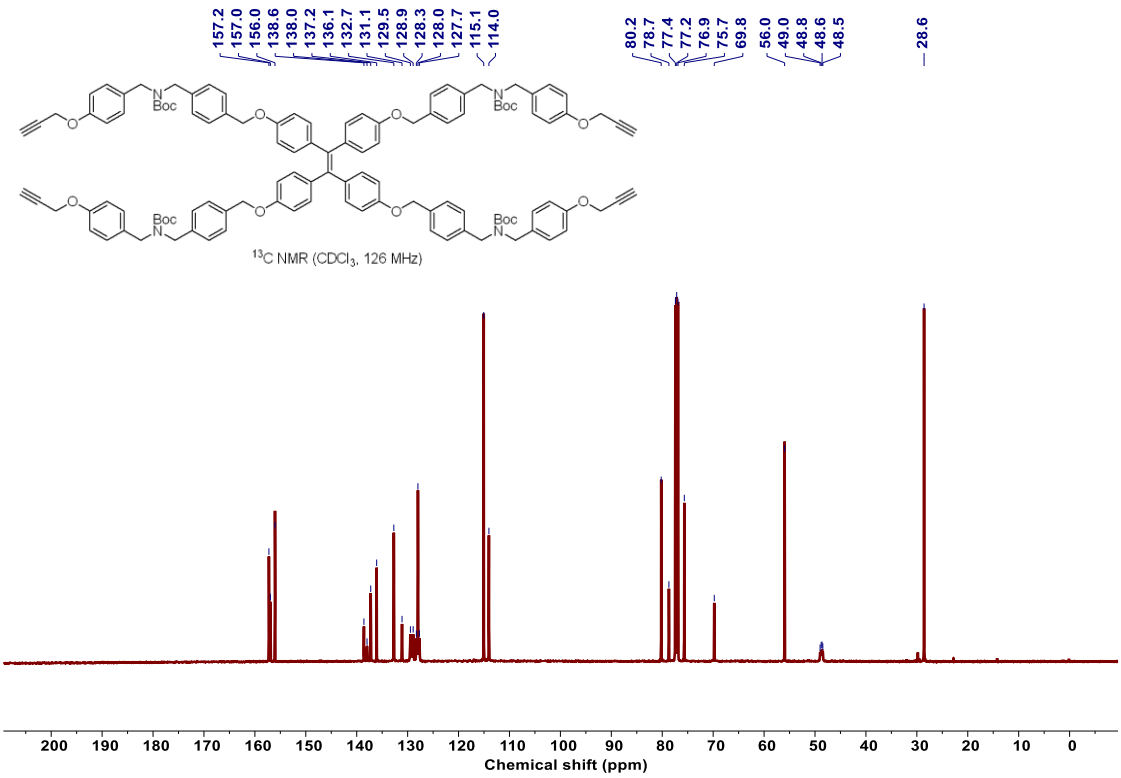

Compound 5: HRMS (ESI, $[M+Na]^+$)

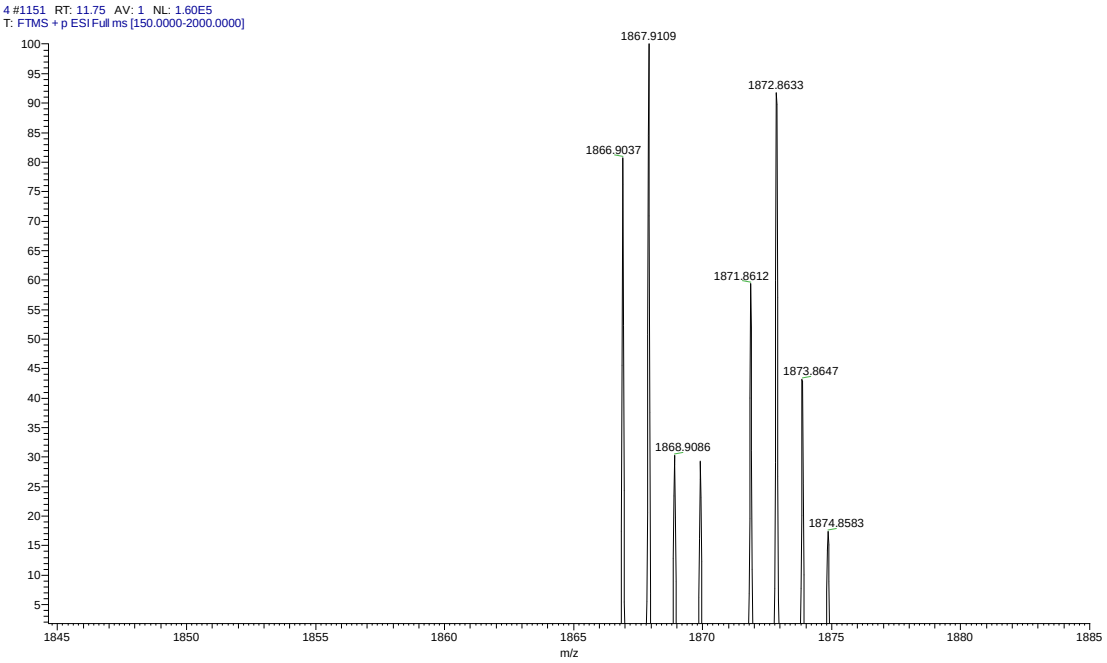

A_{TPE}: ^{1}H NMR (500 MHz, DMSO-d_6)

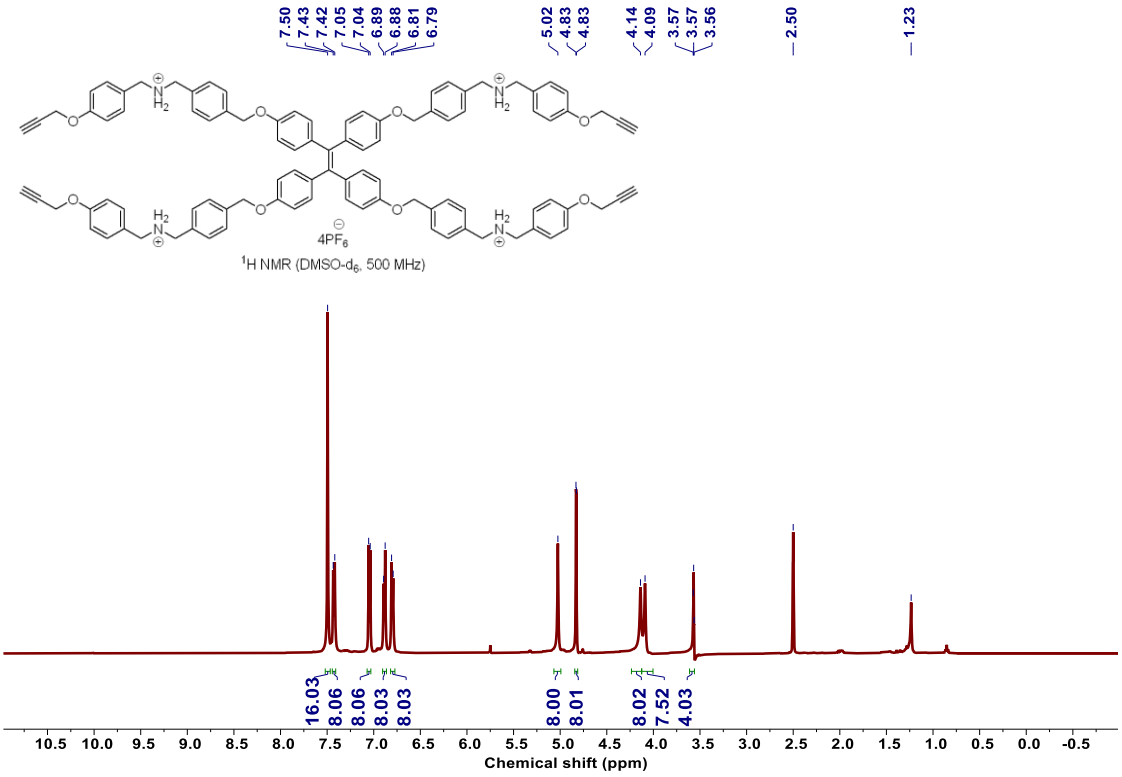

A_{TPE}: ^{13}C NMR (126 MHz, DMSO-d_6)

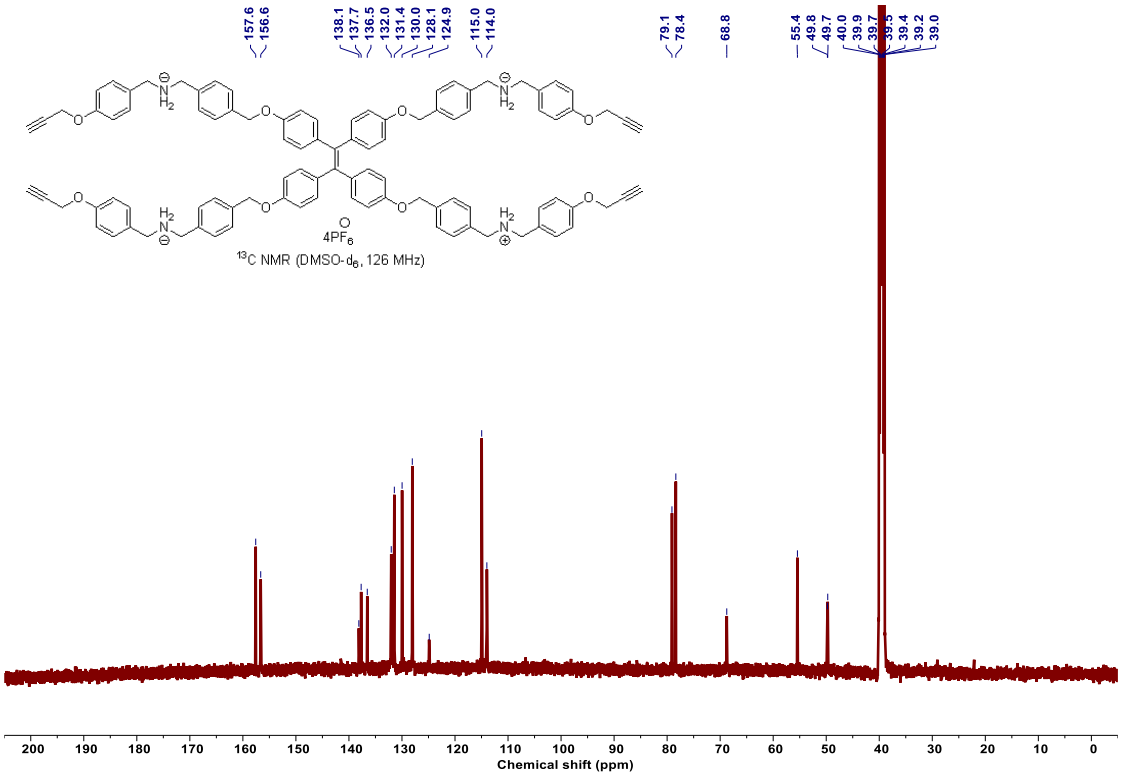

A_{TPE}: HRMS (ESI, $[M - 4PF_6^-]^{4+}$)

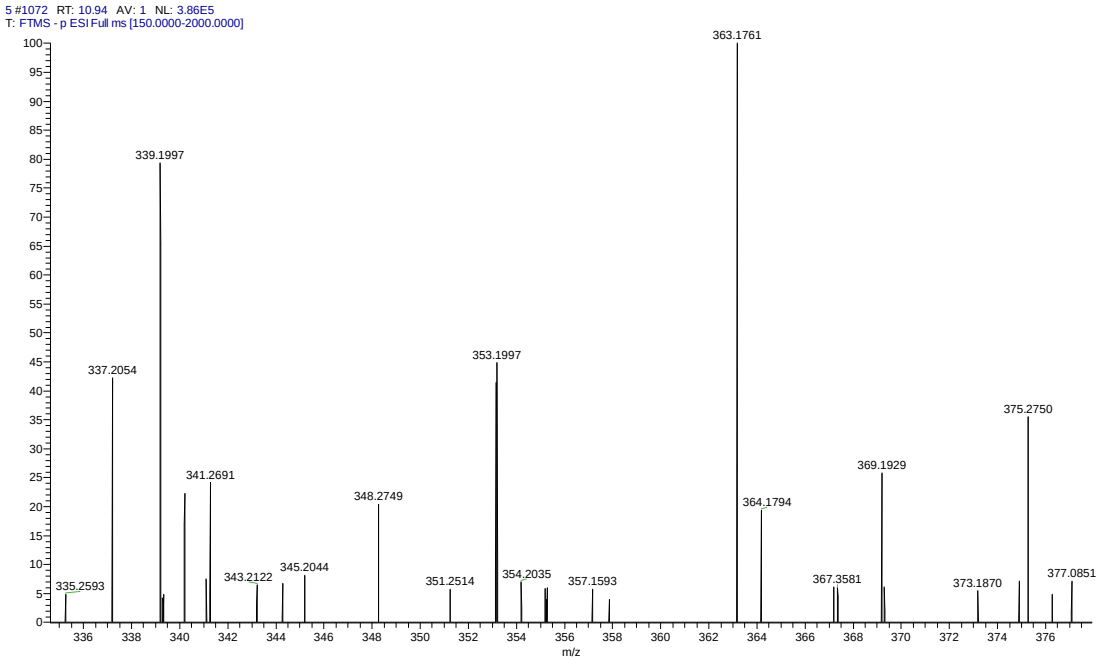

$A_{TPE}S$: ^{1}H NMR (500 MHz, CD_3CN)

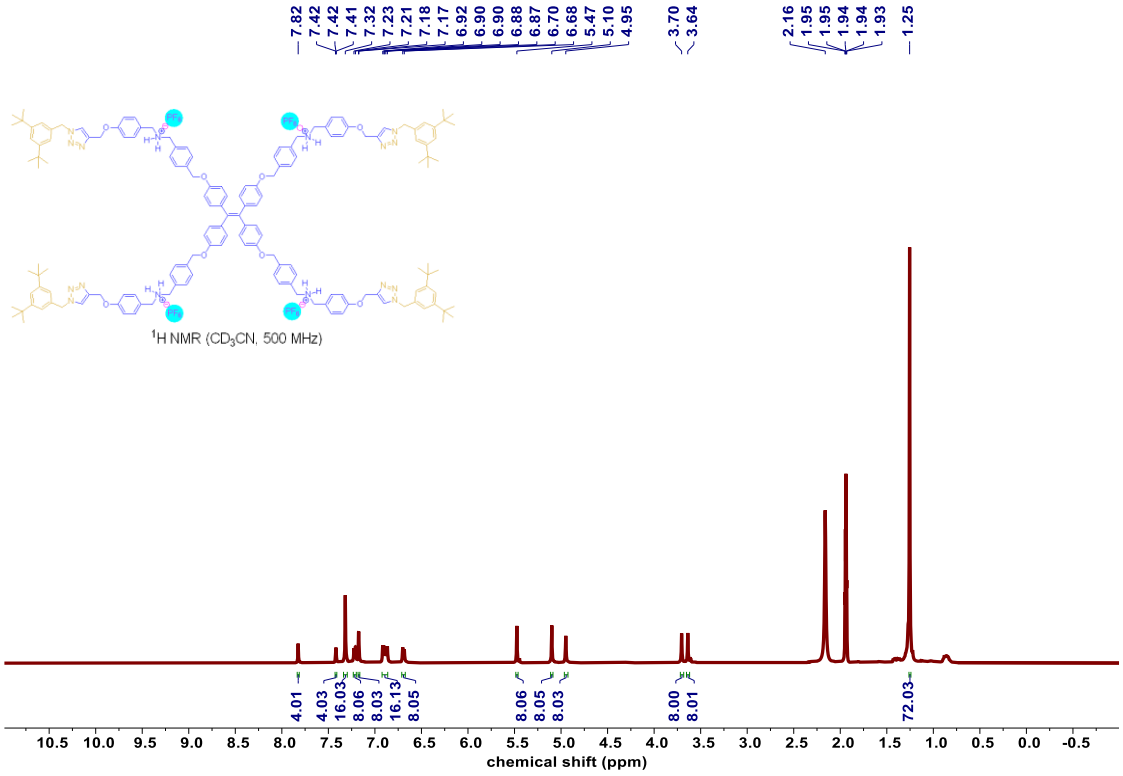

$A_{TPE}S$: ^{13}C NMR (126 MHz, CD_3CN)

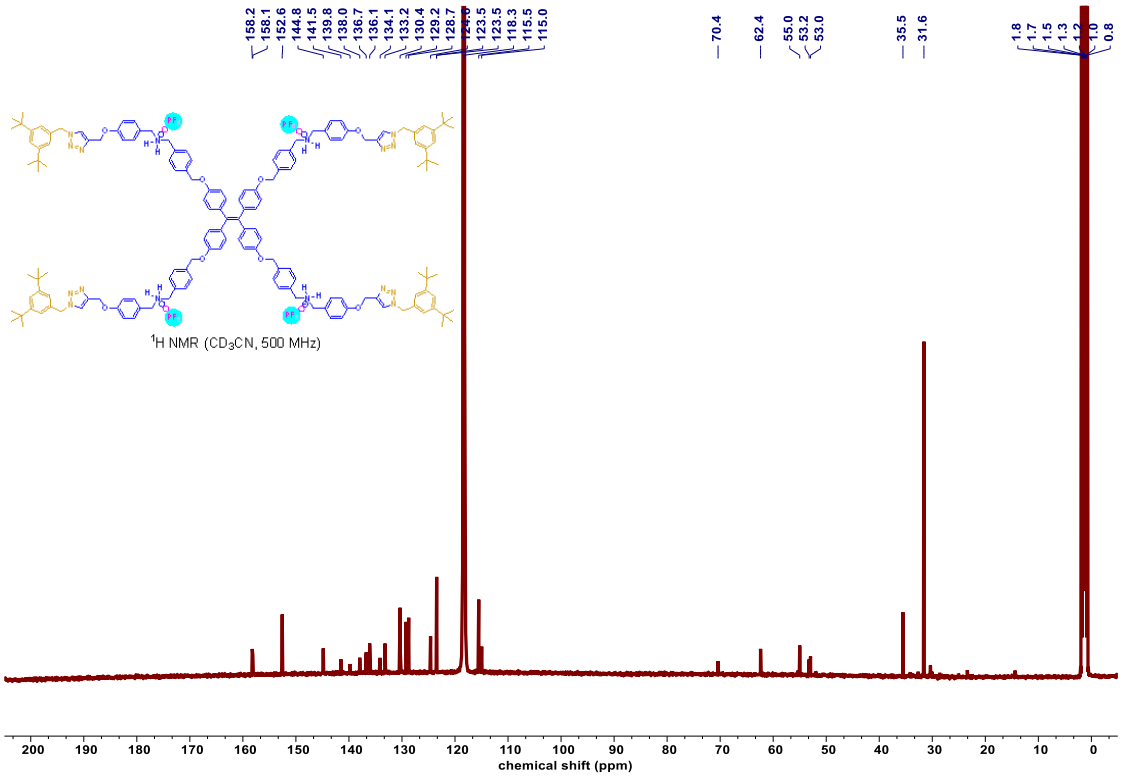

$A_{TPE}S$: HRMS (MALDI, $[M-4PF_6^- -3H]^+$)

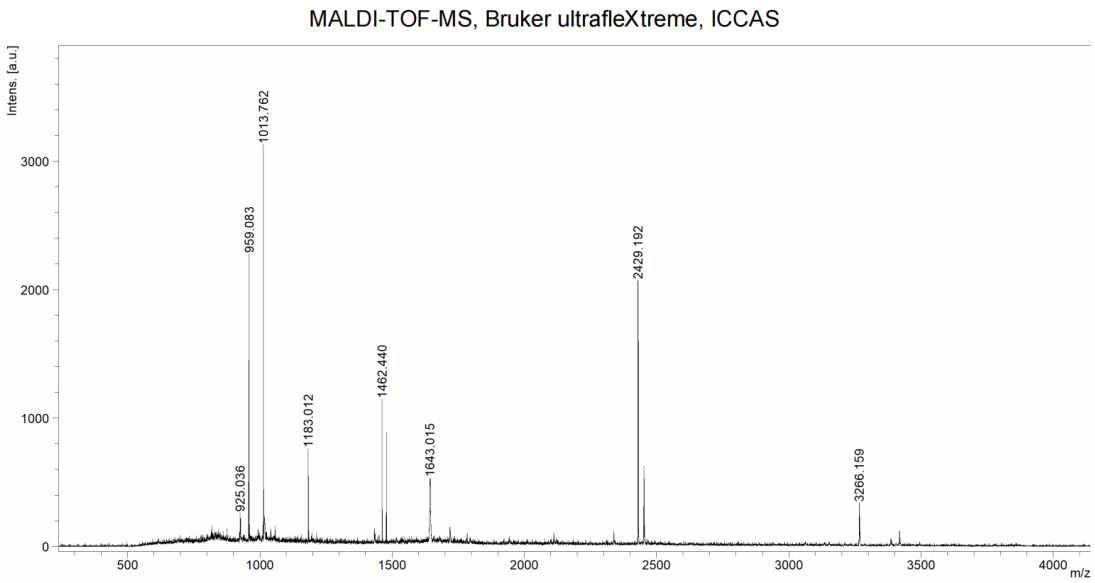

[5]Rotaxane R_{5F}: ^{1}H NMR (500 MHz, CD_3CN)

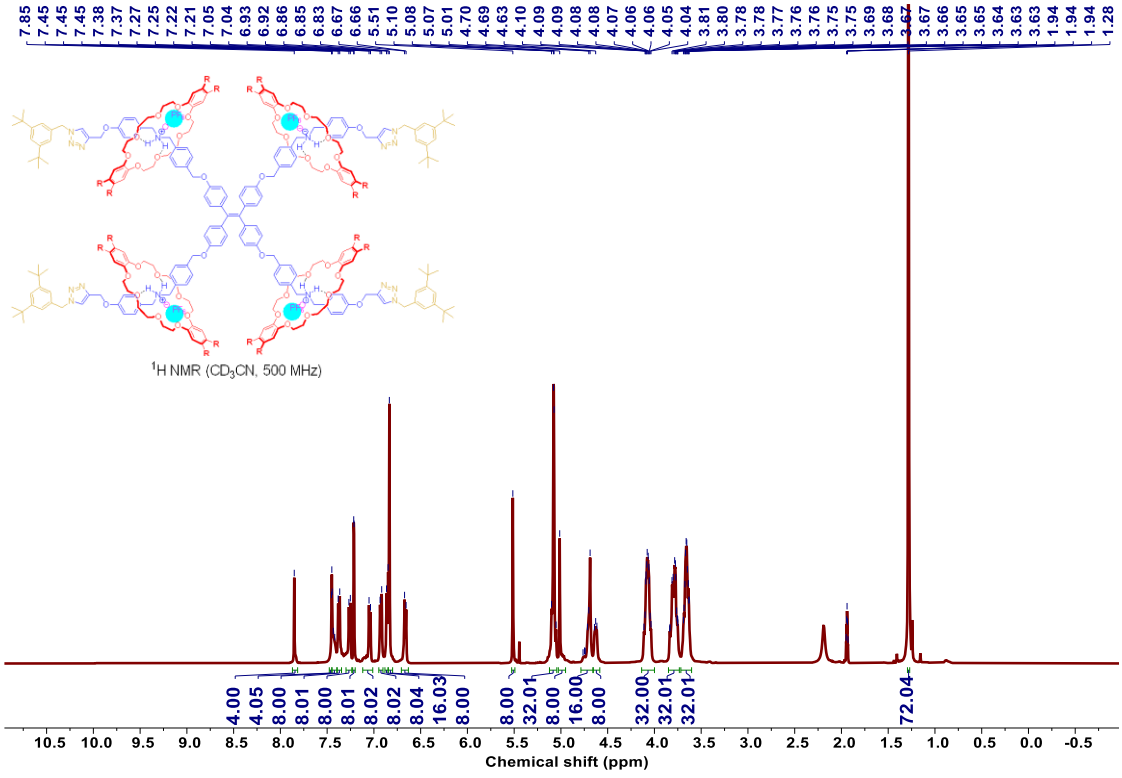

[5]Rotaxane R_{5F}: ^{19}F NMR (471 MHz, CD_3CN)

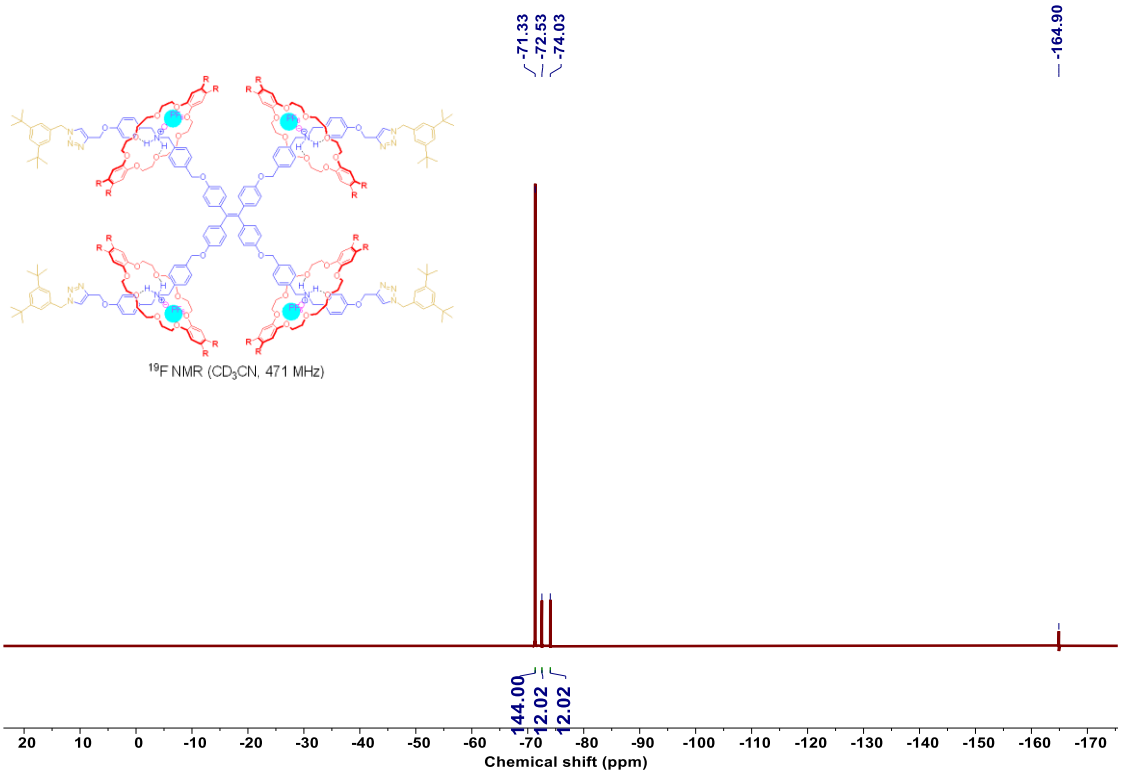

[5]Rotaxane R_{5F}: ^{13}C NMR (126 MHz, CD_3CN)

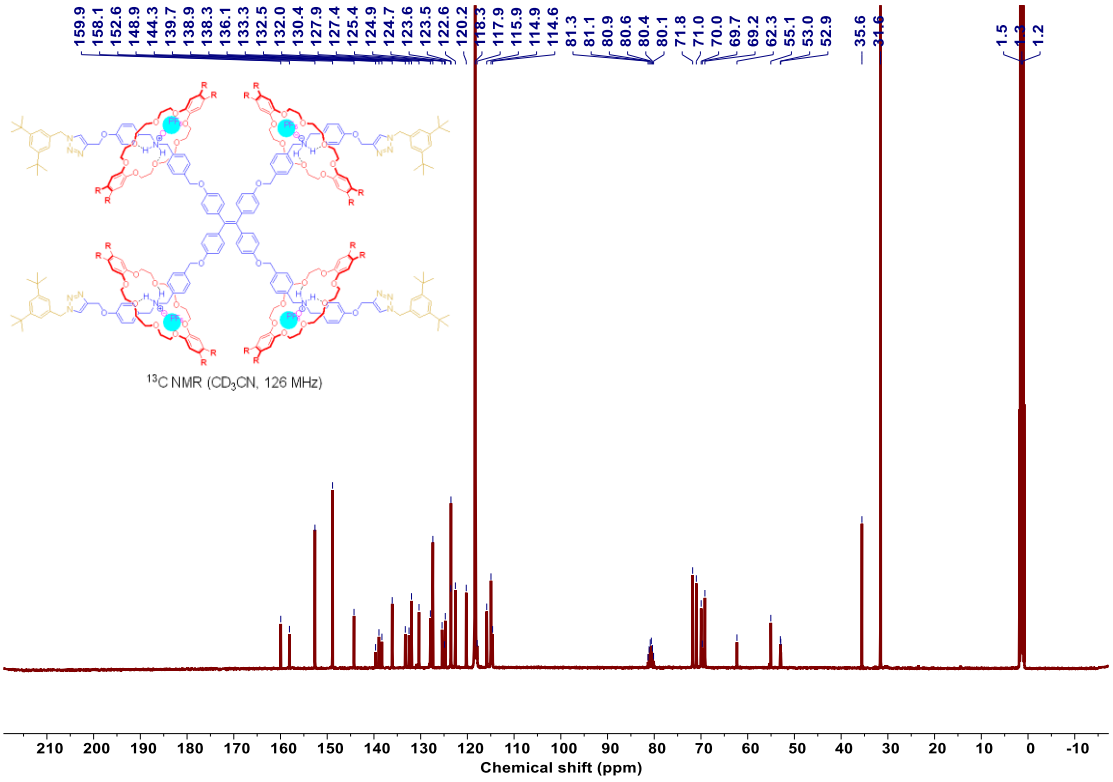

[5]Rotaxane R_{5F}: HRMS (MALDI, $[M–4PF_6^-–3H]^+$)

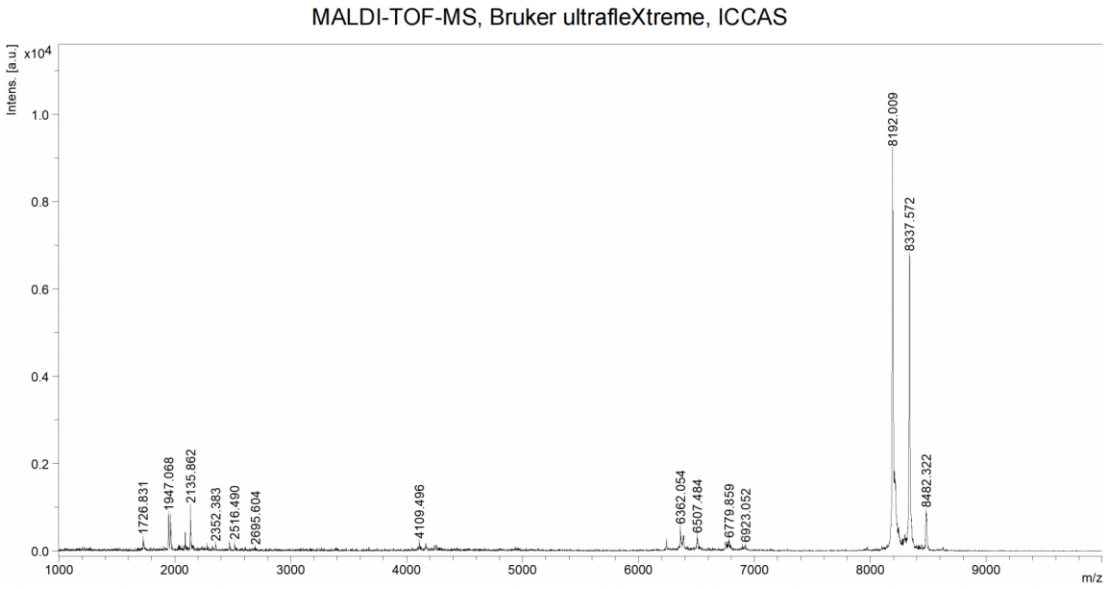

[5]Rotaxane R_{5H}: ^{1}H NMR (500 MHz, CD_3CN)

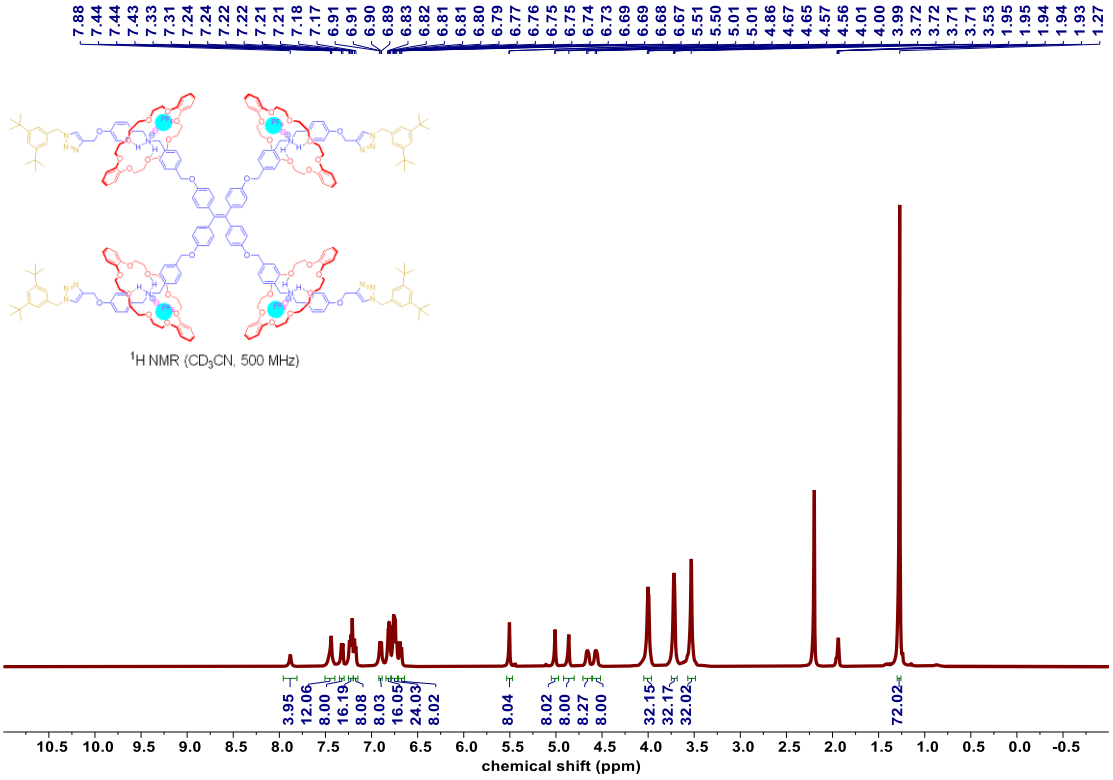

[5]Rotaxane R_{5H}: ^{19}F NMR (471 MHz, CD_3CN)

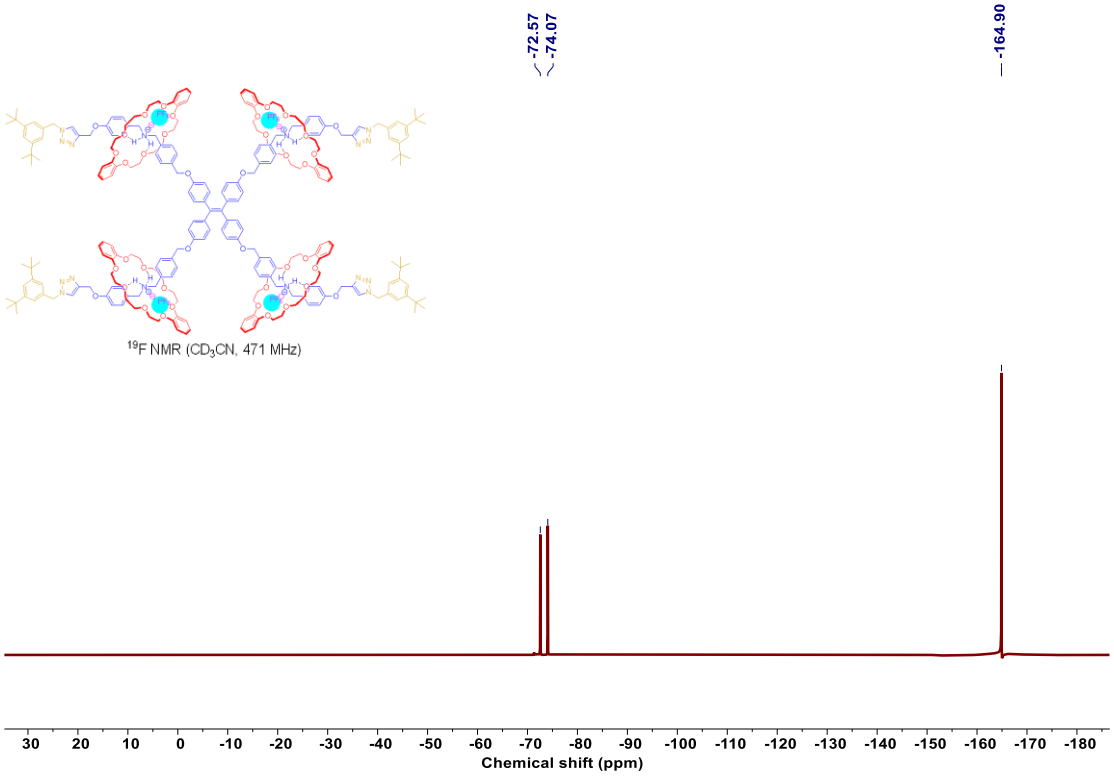

[5]Rotaxane R_{5H}: ^{13}C NMR (126 MHz, CD_3CN)

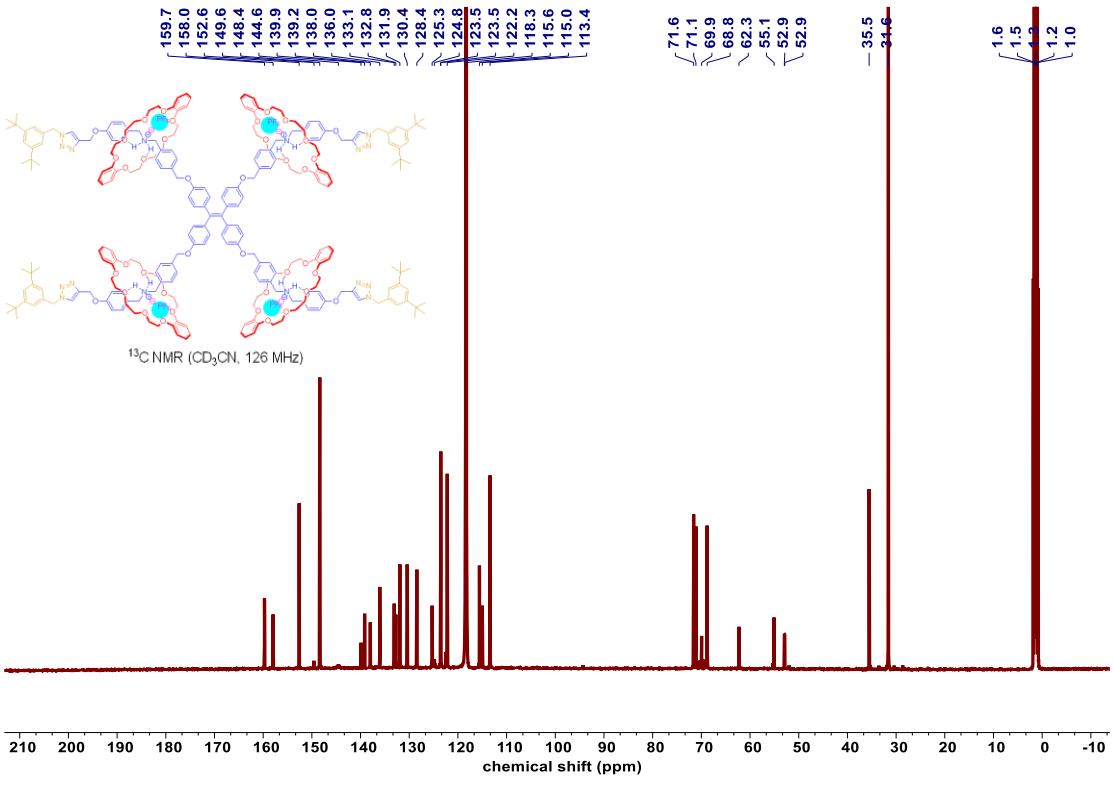

[5]Rotaxane R_{5H}: HRMS (MALDI, $[M–4PF_6^-–3H]^+$)

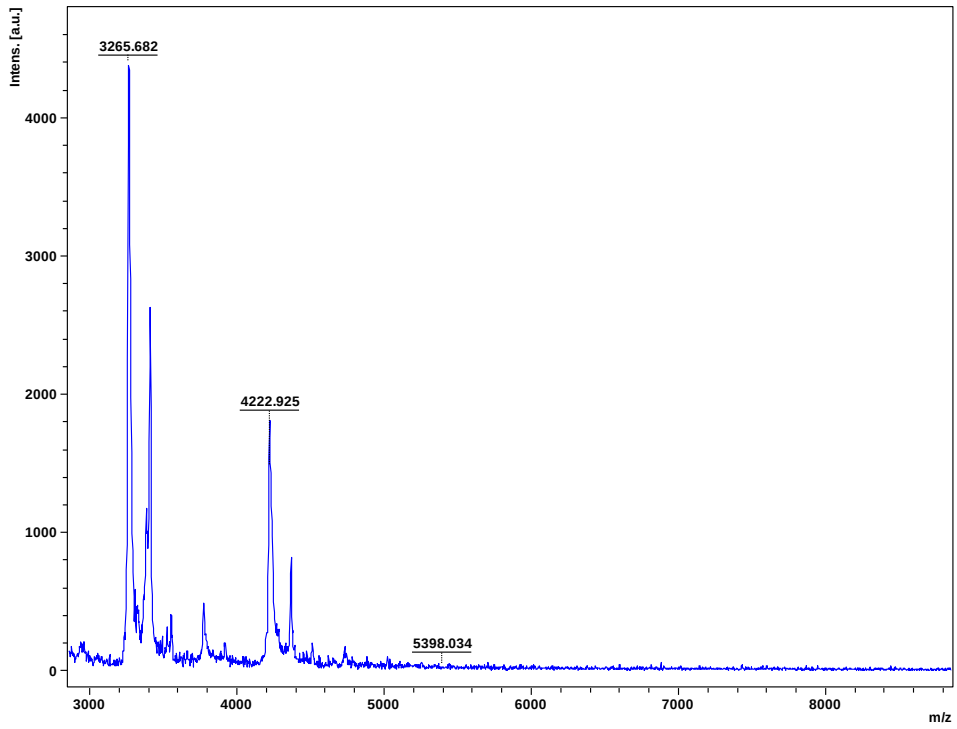

[5]Rotaxane R'_{5F}: ^{1}H NMR (500 MHz, CD_3CN)

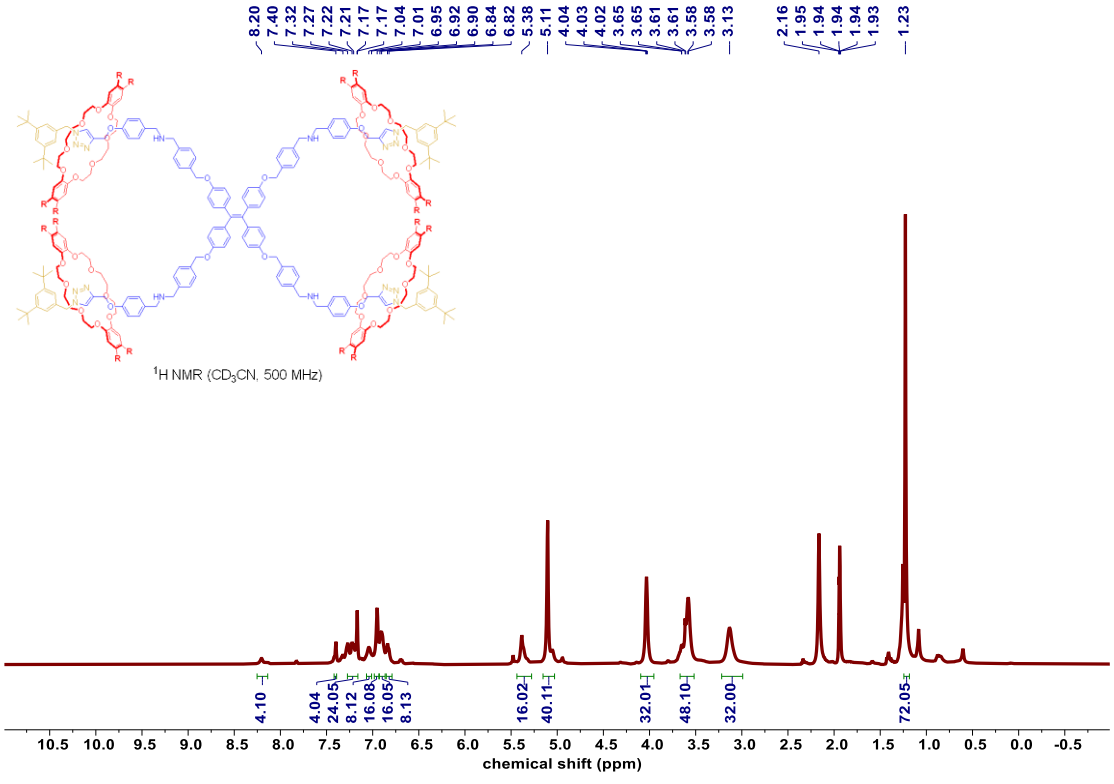

[5]Rotaxane R′$_{5F}$: ^{19}F NMR (471 MHz, CD_3CN)

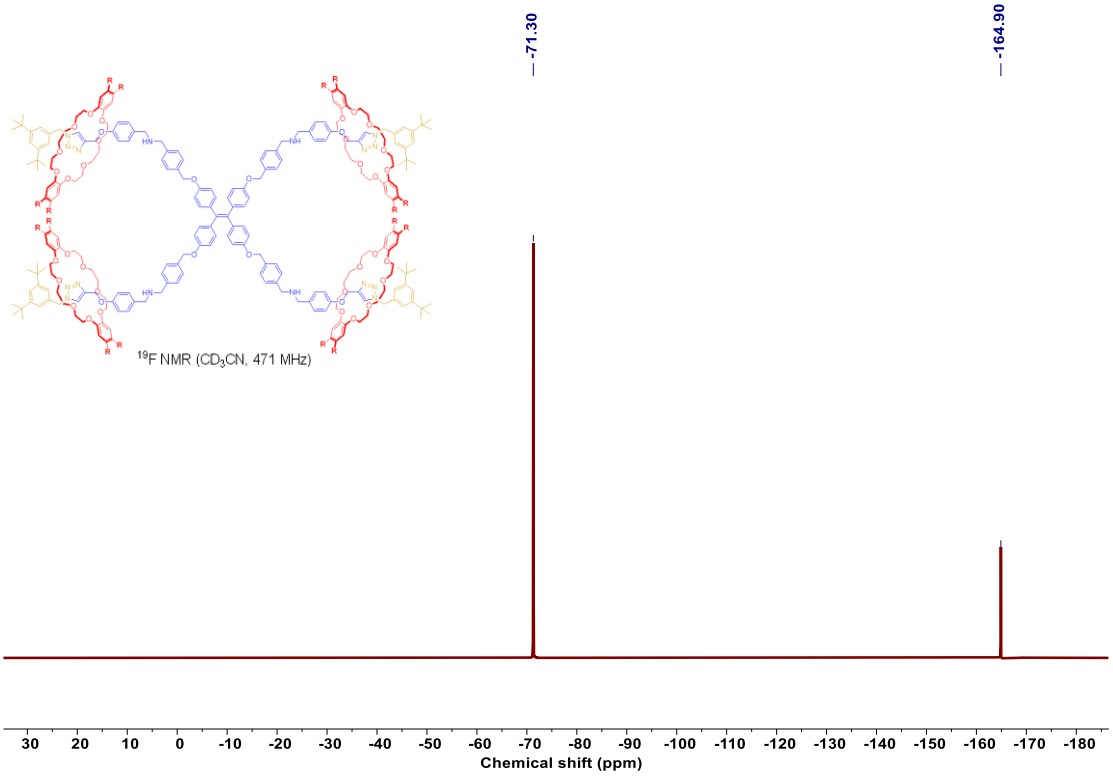

[5]Rotaxane R′$_{5F}$: ^{13}C NMR (126 MHz, CD_3CN)

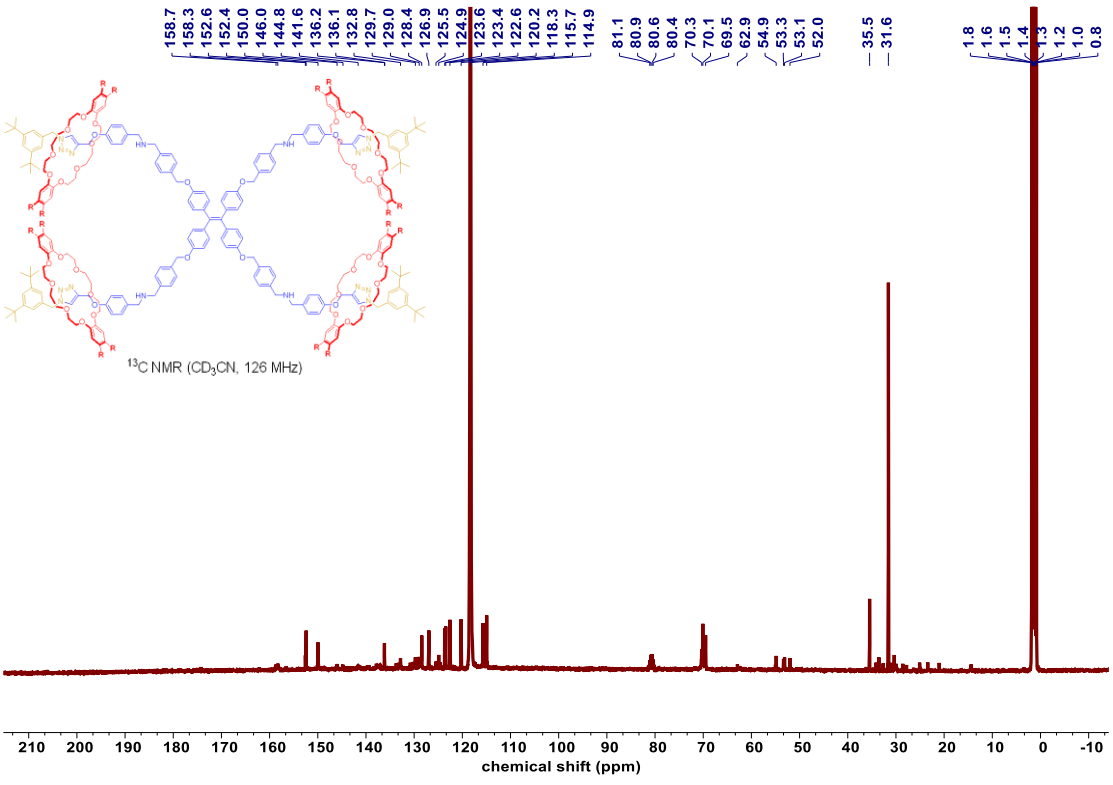

[5]Rotaxane R′$_{5F}$: HRMS (MALDI, [M+H]$^+$)

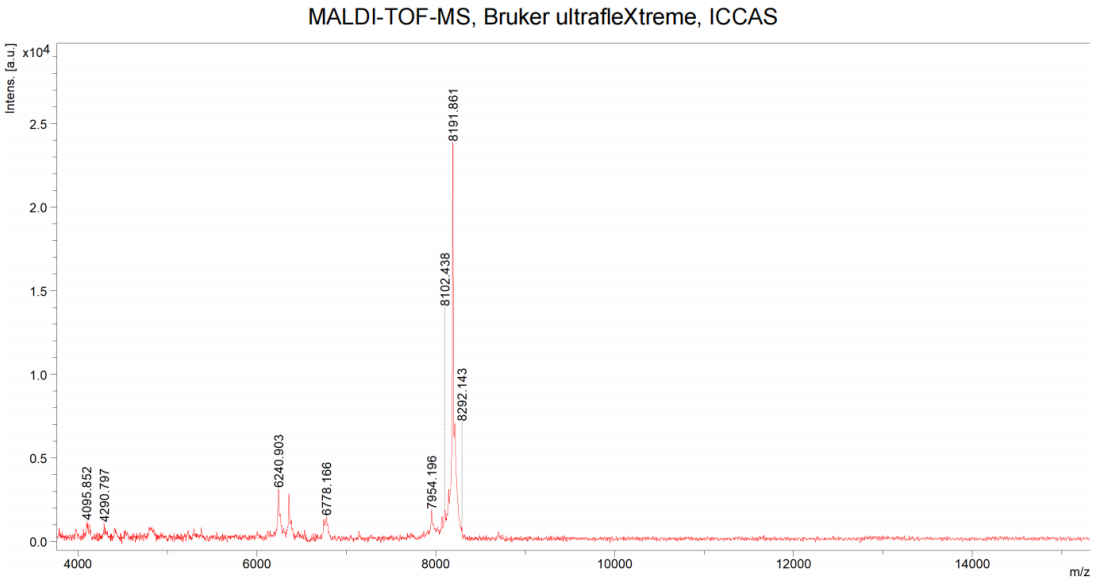

[5]Rotaxane R′$_{5H}$: ^{1}H NMR (600 MHz, CD_3CN)

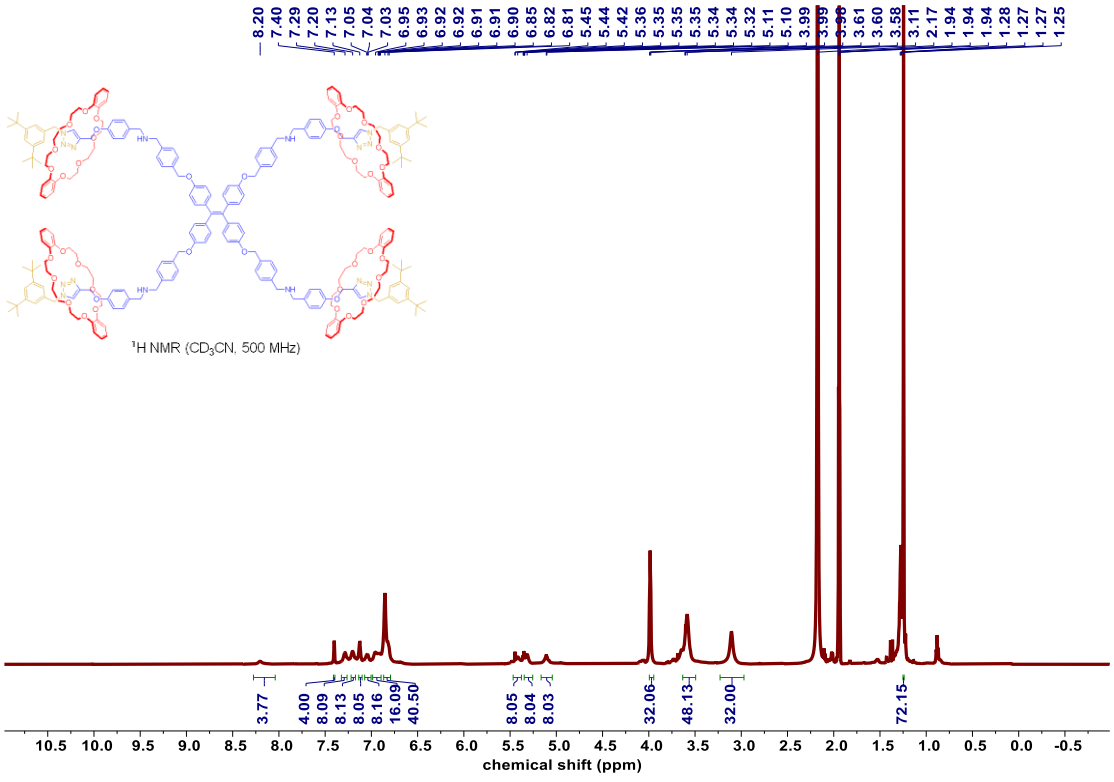

[5]Rotaxane R′$_{5H}$: ^{13}C NMR (126 MHz, CD_3CN)

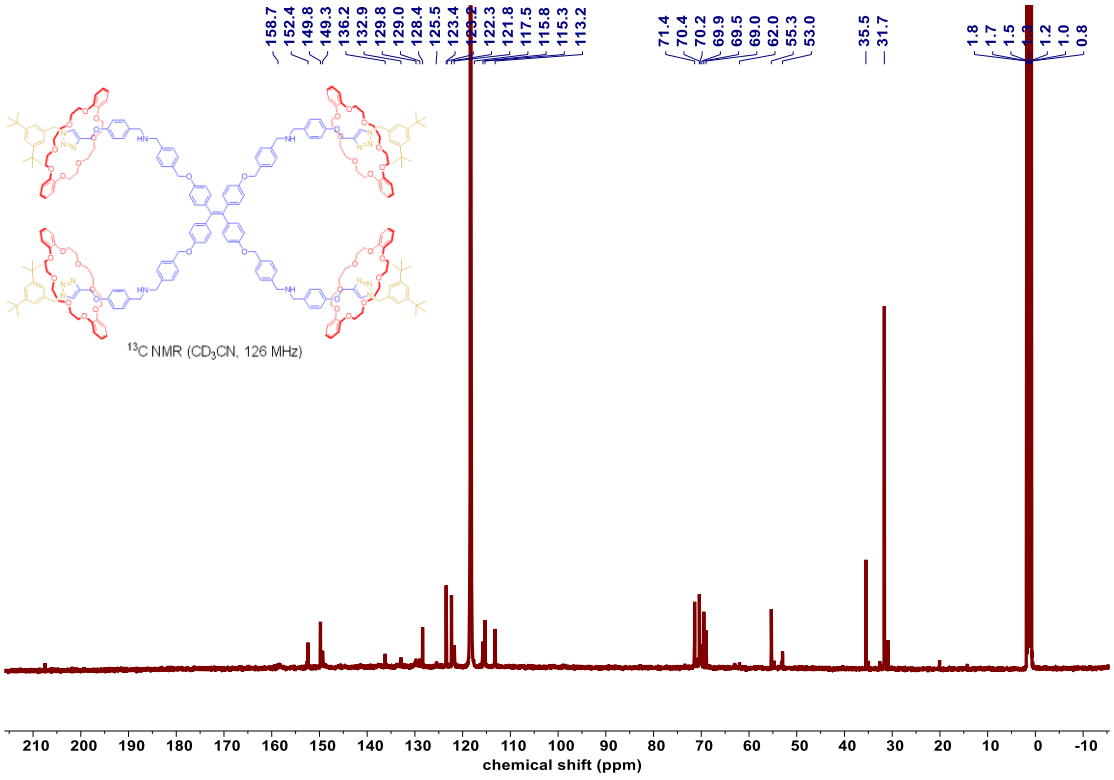

[5]Rotaxane R′$_{5H}$: HRMS (MALDI, $[M+H]^+$)

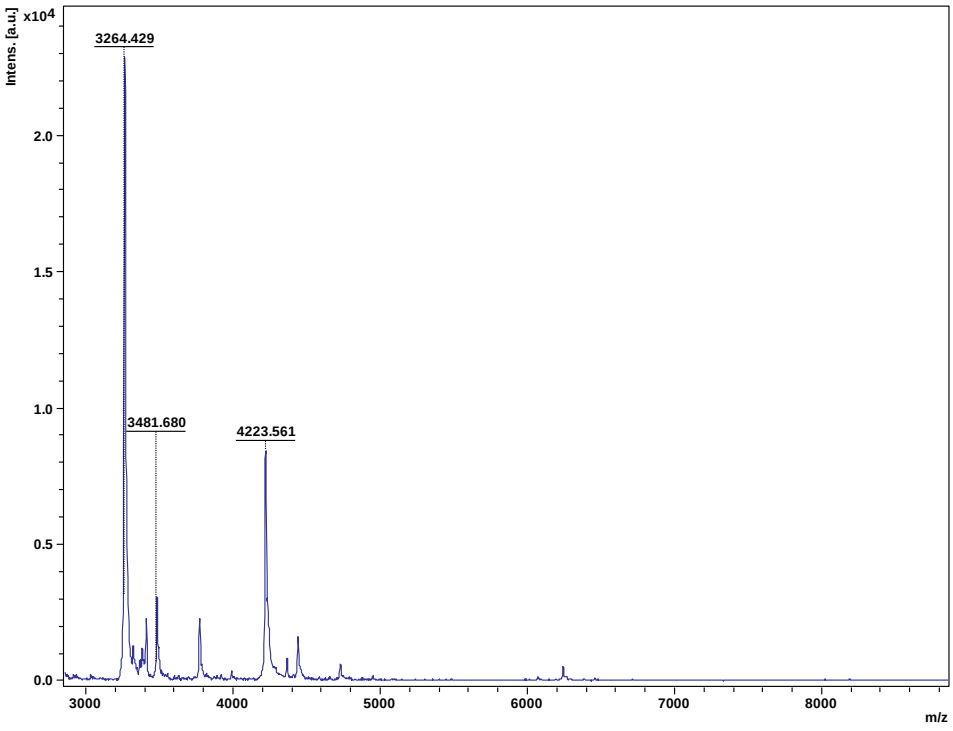

Nanoemusion R_{5F}NPs: **^{19}F NMR (471 MHz, D_2O)**